Dissertation

Programming endothelial dysfunction in diabetic pregnancies

Francisca Isidora DÍAZ PÉREZ

for the academic degree of

Doctor of Philosophy

(PhD)

at the

Medical University of Graz

Department of Obstetrics and Gynecology

under supervision of

ao.Univ.-Prof. Dr. Gernot DESOYE

&

Ass.Prof.in Priv.-Doz.in Dr.in Ursula HIDEN

2016

Declaration

I hereby declare that this thesis is my own original work and that I have fully acknowledged by name all of those individuals and organizations that have contributed to the research for this thesis. Due acknowledgment has been made in the text to all other material used. Throughout this thesis and in all related publications I followed the guidelines of "Good Scientific Practice and Ombuds Committee at the Medical University of Graz".

_____

Francisca Isidora Díaz Pérez

Graz, August 2016

Aknowledgments

I would like to express my gratitude to Gernot Desoye for the opportunity to perform my PhD studies under his supervision, for his endless enthusiasm, his guidance through these years and the challenging, but fruitful discussions.

My most sincere thanks to Ursula Hiden for her academic and personal guidance, for her support and motivation throughout my PhD.

Special thanks to thank Monika Holler for her help with administrative issues and to all my colleagues from the Forschungslabor-team for helping me with their advice and for the great working atmosphere that I experienced during these years.

I would like to thank to Dr. Thomas N. Wight from the Benaroya Research Institute at Virginia Mason in Seattle, WA, and to Dr. Pieter Koolwijk from the VU University Medical Center in Amsterdam, for the new techniques that I learned during my stay and for the kind welcome to their laboratories.

And, I would also like to thank the Austrian Science Fund FWF (W1241) and the Medical University Graz for supporting my PhD through the PhD Program Molecular Fundamentals of Inflammation (DK-MOLIN). Thanks to the European Foundation for the Study of Diabetes (EFSD) for funding my research stay in Amsterdam through the Albert Renold Fellowship Program.

Table of Contents

Abbreviations & Definition

[^{35}S]-sulphate:	Sulphate labeled with radioactive sulphate 35
[^{3}H]-L-arginine:	Titrated L-arginine
[^{3}H]-L-citrulline:	Titrated L-citrulline
ACH-3P:	First trimester human trophoblast cell line
AEC:	Arterial endothelial cells
ANOVA:	Analysis of variance
APEX:	Apurinic/apyrimidinic endodeoxyribonuclease
AU:	Arbitrary units
BCA:	Bicinchonic acid assay
BMI:	Body mass index
C:	Control
CBS:	Cord blood serum
CCND2:	Cyclin-D2
CD:	Cluster of differentiation
CDC47/mcm7:	Mini-chromosome maintenance complex component 7
CDK:	Cyclin dependent kinase
CDKN1B/p27:	Cyclin-dependent kinase inhibitor 1B (p27, Kip1) protein
cDNA:	Complementary deoxyribonucleic acid
CRP:	C-reactive protein
CVD:	Cardiovascular diseases
D:	Gestational diabetic
DAF:	Diaminofluorescein
DAF-FM:	4-amino-5-methylamino-2',7'-difluorofluorescein

DAPI:	4',6-diamidino-2-phenylindole
DEAE-sephacel:	Diethylaminoethyl-sephacel
DMEM:	Dulbecco's modified Eagle's medium
DNA:	Deoxyribonucleic acid
DNMT:	Deoxyribonucleic acid methyl transferases
EBM:	Endothelial basal medium
ECM:	Extracellular matrix
EDTA:	Ethylenediaminetetraacetic acid
EGF:	Epidermal growth factor
EGM-MV:	Endothelial cell growth medium
EHS:	Engelbreth-Holm-Swarm mouse sarcoma
ELISA:	Enzyme-linked immunosorbent assay
eNOS:	Endothelial nitric oxide synthase
EP300:	E1A Binding Protein P300
FACS:	Fluorescence-activated cell sorting
FANCC:	Fanconi anemia complementation group C
FBN1:	Fibrillin1
FBS:	Fetal bovine serum
FC:	Fold change
FCS:	Fetal calf serum
FGF:	Fibroblast growth factor
FITC:	Fluorescein isothiocyanate
FTT:	First trimester trophoblasts
GADD45B:	Growth arrest and DNA damage inducible β

GAG:	Glycosaminoglycan
GAPDH:	Glyceraldehyde 3-phosphate dehydrogenase
GDM:	Gestational diabetes mellitus
H_2O:	Dihydroxide
HBC:	Hofbauer cells
HBSS:	Hank's balanced salt solution
HEPES:	4-(2-hydroxyethyl)-1-piperazineethanesulfonic acid buffer
HOPE:	Hepes glutamic acid buffer mediated organic solvent protection effect
HPRT1:	Hypoxanthine phosphoribosyltransferase 1
HRP:	Horseradish peroxidase
HS:	Human serum
hSMC:	Human smooth muscle cells
HUVEC:	Human umbilical vein endothelial cells
ICAM-1:	Intercellular adhesion molecule 1
IF:	Immunofluorescence
IGF1R:	Insulin-like growth factor I
IgG:	Immunoglobulin G
IHC:	Immunocytochemistry
IL:	Interleukin
LFA:	Lymphocyte function-associated antigen 1
L-NAME:	L-NG-Nitroarginine methyl ester
MFI:	Mean fluorescence intensity
mRNA:	Messenger ribonucleic acid
NaCl:	Sodium chloride

NGT:	Normal glucose tolerance
NO:	Nitric oxide
NOS:	Nitric oxide synthases
NOS3:	Endothelial nitric oxide synthase (also mentioned as eNOS)
O_2:	Oxygen
oGTT:	Oral glucose tolerance test
PBS:	Phosphate-buffered saline
PFA:	Paraformaldehyde
PG:	Proteoglycans
RB:	Retinoblastoma
RIPA:	Radio-immunoprecipitation assay
RNA:	Ribonucleic acid
RNA:	Ribonucleic acid
RT-qPCR:	Reverse transcription- quantitative polymerase chain reaction
SDS-PAGE:	Sodium dodecyl sulfate-polyacrylamide gel electrophoresis
SEM:	Standard error of the mean
sE-selectin:	Soluble endothelial selectin
sICAM-1:	Soluble intercellular adhesion molecule 1
siRNA:	Small interfering ribonucleic acid
SmBM:	Smooth muscle basal medium
SMC:	Smooth muscle cells
SmGM:	Smooth muscle growth medium
SN:	Supernatant
sVCAM-1:	Soluble vascular cell adhesion molecule 1

T2DM:	Type 2 diabetes mellitus
TBE:	Tris-borate-EDTA
TBS:	Tris-buffered saline
TGFβ1:	Transforming growth factor β1
TGFβI:	Transforming growth factor β induced
TNFα:	Tumor necrosis factor α
TPT:	Term placental tissue
TT:	Term trophoblasts
VCAM-1:	Vascular cell adhesion molecule 1
VCAN:	Versican
VEC:	Venous endothelial cells
VEGF:	Vascular endothelial growth factor
YWHAH:	Tyrosine 3-monooxygenase/tryptophan 5-monooxygenase activation protein Eta (14.3.3 η)

Zusammenfassung

Schwangerschaftsdiabetes oder Gestationsdiabetes (GDM) ist eine mütterliche Glukosestörung, die zu einem erhöhten Risiko für kardiovaskuläre Erkrankungen der Mutter und des Kindes führt. Das Endothel der feto-plazentären Vaskulatur ist der Hyperglykämie und dem pro-inflammatorischen Milieu von GDM ausgesetzt. Wir erstellten die Hypothese, dass der Phänotyp arterieller Endothelzellen aus der menschlichen Plazenta nach diabetischen Schwangerschaften verändert ist.

Hierzu wurden primäre arterielle Endothelzellen aus humanen Plazenten nach gesunden (Kontroll-AEC), sowie nach GDM Schwangerschaften (GDM-AEC) isoliert und kultiviert. Das Transkriptom wurde mittels RT-qPCR ausgewertet. Zielproteine wurden durch ELISA, Immunoblot, Immunfluoreszenz (IF) und / oderImmunhistochemie (IHC) evaluiert. Das angiogene Potential der untersuchten Zellen wurde im 3D Tube-Formation Assay analysiert.

Die wichtigsten Ergebnisse dieser Studie waren: 1) Die mRNA Expression von eNOS und die NO-Bioverfügbarkeit in AEC waren in GDM AEC unverändert. 2) GDM führt zu einem verringerten Level von ICAM-1. 3) Die Zellzyklus-Regulatoren CDK4 und Cyclin-D2 waren nach GDM verändert und auch die Tube-Formation war reduziert. 4) GDM erhöhte den mRNA-Spiegel von allen Versican Isoformen (V0, V1, V2 und V3). Der ELISA zeigte, dass alle Versican Isoformen in Überständen von GDM AEC verringert sind. Es konnten jedoch keine Veränderungen im Zelllysat nachgewiesen werden. Die Versican V0 Konzentration war im Zelllysat von GDM AEC erhöht, aber in den Überständen unverändert. Mittels Immunoblot und der IF war V0 in kultivierten AEC nicht nachweisbar. Diese Ergebnisse deuten auf Veränderungen in der Expression, Translation und Sekretion der Versican Isoformen bei GDM hin.

Die Veränderungen im extrazellulären Matrixprotein Versican, in den Zellzyklus-Regulatoren CDK4 und Cyclin-D2, und im angiogenen Potential von Plazenta-Endothelzellen nach GDM korrelieren mit den Veränderungen in der DNA Methylierung, welche in vorherigen Experimenten identifiziert wurden. Das deutet darauf hin, dass *in utero* eine epigenetische Programming von Plazenta-Endothelzellen stattfindet. Darüber hinaus scheinen diese Veränderungen

kompensiert zu werden, da die NO Verfügbarkeit, sowie eNOS Expression unbeeinflusst sind, und ICAM-1 sogar reduziert ist. Diese Kompensation, beziehungsweise die Stabilität der Plazenta, weist auf eine schützende Rolle des Plazenta-Endothels bei Schwangerschaftsdiabetes hin.

Abstract

Gestational diabetes mellitus (GDM) is a maternal glucose disorder that leads to an increased risk of cardiovascular disease (CVD) for both, mother and the offspring. In GDM, the endothelium of the feto-placental vasculature is exposed to hyperglycaemia and a pro-inflammatory environment. We hypothesized that human placental arterial endothelial cells of healthy and GDM pregnancies differ in their phenotype as a result of epigenetic modifications caused by the low-grade pro-inflammatory environment of GDM.

For this purpose, primary arterial endothelial cells were isolated from human term placentas of healthy (control AEC) and GDM pregnancies (GDM AEC) and cultured. Endothelial functions, such as cell adhesion molecule expression for macrophage attachment, nitric oxide synthesis for vascular tone regulation, and angiogenesis including proliferation were investigated. Transcriptome was analyzed by RT-qPCR. Target proteins were investigated by ELISA, immunoblot, immunofluorescence and/or immunohistochemistry. Angiogenic potential of the cells was evaluated by 3D tube-formation assay after seeding cells on top of fibrin matrices.

The main findings of this study were: 1) eNOS mRNA expression and NO-bioavailability were unchanged in AEC from control and GDM placentas. 2) GDM causes decreased levels of ICAM-1 and unaltered levels of VCAM-1 and E-selectin in AEC. 3) GDM altered CDK4 and cyclin-D2 transcript and protein levels, together with decreased angiogenic potential of GDM AEC compared to control AEC. 4) GDM increased mRNA levels of versican (V0, V1, V2 and V3). ELISA showed decreased levels of all forms of versican in supernatant of GDM AEC and no change in cell lysate, while versican V0 was increased in cell lysate of GDM AEC and unaltered in supernatant. Immunoblot and immunofluorescence (IF) failed to detect versican V0 in cultured AEC. These data indicate changes in expression, translation and secretion of different isoforms of versican.

Alterations found in extracellular matrix protein versican, in cell cycle regulators CDK4 and cyclin-D2, and in the angiogenic potential of AEC after GDM correlate with DNA methylation observed previously in our lab, suggesting *in utero*

programming of AEC. Moreover, these changes seem to be compensated with unchanged NO bioavailability and eNOS transcript expression, together with decreased levels of ICAM-1 and unaltered levels of VCAM-1 and E-selectin, which appear to have a protective role of the placenta in GDM.

Introduction

Placenta

The placenta is a highly specialized organ for the development and growth of the embryo and fetus during pregnancy, which provides nutrients and oxygen to the fetus and removes respiratory gases and metabolic wastes (Rama and Rao 2003). The placenta is also involved in the protection of the fetus from certain xenobiotic molecules, infections and diseases of the mother. Moreover, this organ releases hormones into the maternal and fetal circulations affecting pregnancy by modulating fetal metabolism, growth and parturition, within other functions. Throughout pregnancy, the increasing metabolic demands of the growing fetus are sustained by many placental functional modifications (Gude et al., 2004).

The fetal portion of the placenta develops from the chorion, which develops from the cytotrophoblast and syncytiotrophoblast, while the maternal portion is a layer of the endometrium known as decidua. Derivatives of the chorion are in contact with the endometrium, forming fingerlike projections known as the *chorionic villi* on its surface as shown in **Figure 1**. The *chorionic villi* connect with the endometrium and the maternal circulation, yet the fetal and the maternal circulation systems remain separate (Piñon, 2002).

Feto-placental endothelium

The endothelium is a continuous monolayer formed by endothelial cells interconnected by different types of adhesive molecules and structures or cell-cell junctions (Michiels, 2003). Depending on its location, the endothelium will vary in its morphology and functional heterogeneity through differenced expression of a variety of molecules, such as pro- and anticoagulant factors, and by the presence of intercellular interactions and contractility. These properties are essential for adjusting the endothelial function and maintaining homeostasis in response to local alterations (Chistiakov et al., 2015).

During placental development, vasculogenesis and angiogenesis result in the formation of a complex network of vessels, a process controlled by various growth factors, cytokines and oxygen (Wadsack et al., 2012).

The feto-placental vasculature, unlike other vascular beds is not subject to autonomic regulation, but to humoral mediators, many of which are synthesized locally by endothelial cells, regulating placental vascular resistance. Feto-placental endothelial cells play a central role in angiogenesis and vasomotor tone regulation. Therefore, understanding their role in placental vascular biology is of great importance for the development of new clinically relevant approaches to prevent and treat pregnancy pathologies such as gestational diabetes mellitus (GDM) (Su, 2015).

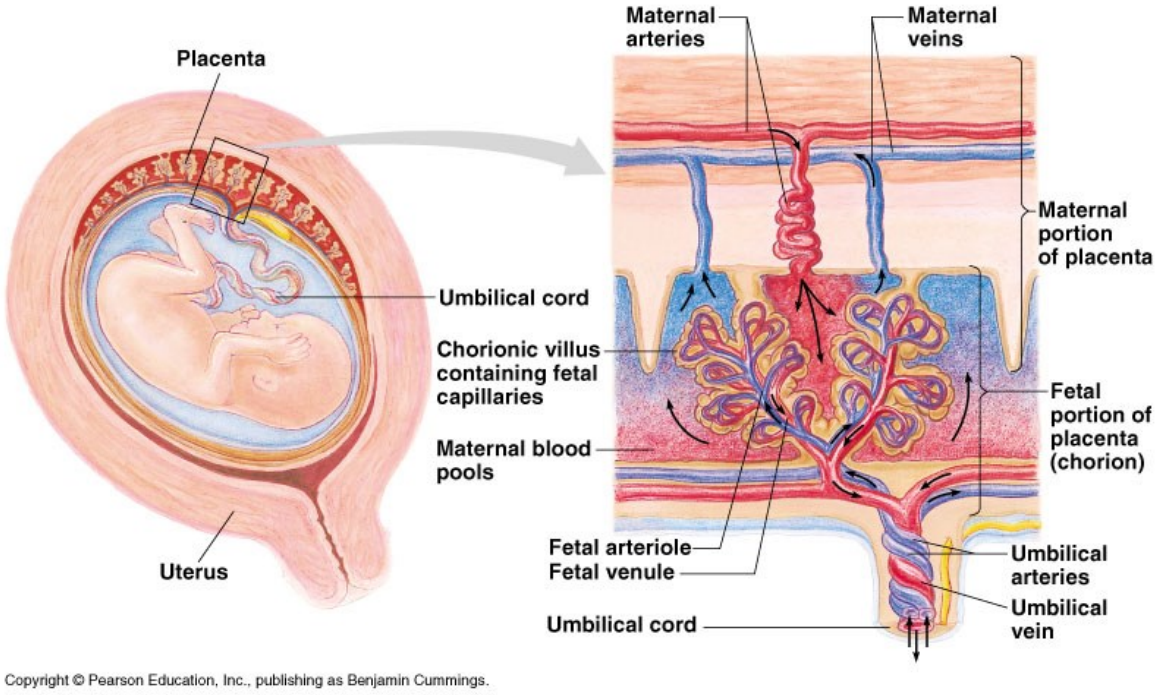

Figure 1. Human placenta.

Illustration of the interaction between the uterus, the placenta, and the fetus during pregnancy (left). Structural scheme of the human placenta indicating the direction of blood flow from mother to the placenta, and fetal blood flow from the placenta to the fetus (right). Download from http://science.kennesaw.edu/~jdirnber/Bio2108/Lecture/LecPhysio/46-17-PlacentalCirculat-AL.jpg (Cummings, 2005).

Endothelial function

Endothelial cells regulate basal vascular tone and vascular reactivity by releasing a variety of vasoactive factors (Pleiner et al., 2007). The inability of endothelial cells to perform their physiological functions leads to impaired function of the endothelium, known as endothelial dysfunction. Dysregulation of several molecules contribute to endothelial dysfunction. However, defect in nitric oxide (NO) synthesis or activity has been proposed as a major mechanism for endothelial dysfunction (Davignon and Ganz, 2004).

Nitric oxide (NO)

In physiological conditions, NO is an essential molecule for endothelial function. This endothelial-derived vasodilator is produced by the conversion of L-arginine into L-citrulline by a family of nitric oxide synthases (NOS). NO plays a key role to maintain the vascular wall in a quiescent state by inhibition of inflammation, cellular proliferation, and thrombosis (Deanfield et al., 2007), by regulating vascular tone and local blood flow, platelet aggregation and adhesion, and leukocyte-endothelial cell interactions (Huang, 2003; Tousolis et al., 2012).

Cell adhesion molecules

Other classical markers of endothelial dysfunction are endothelial cell adhesion molecules, and the most well described are intercellular cell adhesion molecule-1 (ICAM-1), vascular cell adhesion molecule-1 (VCAM-1) and endothelial selectin (E-selectin). Expression of ICAM-1, VCAM-1 and E-selectin in endothelial cells increases via cytokine stimulation, and their major function is to bind ligands present on leukocytes in order to promote leukocyte attachment and trans-endothelial migration. Furthermore, proteolytic cleavage of these adhesion molecules result in release of soluble forms sICAM-1, sVCAM-1 and sE-selectin (Díaz-Pérez et al., 2016).

Angiogenesis

Formation of new blood vessels from pre-existing ones, a process known as angiogenesis, is another important function of endothelial cells. Angiogenesis regulation occurs by the interaction of angiogenic growth factors and cytokines with the endothelium and its surrounding matrix, which is regulated by proteases and adhesion molecules (van Hinsbergh et al., 1999). Angiogenesis plays a central role in development, while in adulthood is limited to the female reproductive system under physiological conditions, and in pathological conditions is involved in tissue repair (van Hinsbergh et al., 2001). During pregnancy, a gradual increase in placental angiogenesis is required to provide adequate nutrients supply to the fetus. Angiogenesis rates accelerate significantly at around the 25th week of gestation, resulting in increased length of the villous vascular tree (Su, 2015).

Gestational diabetes mellitus (GDM)

Gestational diabetes mellitus (GDM) is a glucose intolerance disorder that manifests in the second trimester of gestation and usually resolves after birth. Both, the mother and the growing fetus are affected by GDM. According to the International Diabetes Federation up to 15% of pregnant women worldwide are affected, the prevalence in Europe is 2-6% (Buckley et al., 2012).

The GDM environment is marked by changes in a network of substances in the mother, and therefore, also in the fetus. The fetal GDM environment is characterized by higher levels of glucose, leptin, insulin, adiponectin and other cytokines (Desoye and Hauguel-de Mouzon, 2007). As a consequence of GDM, fetuses exhibit excessive fetal growth, which results in macrosomic infants.

Endothelial function & GDM

Maternal hormonal influences do not affect the feto-placental endothelium directly. However, changes in nutrient supply may alter fetal metabolism and fetal levels of hormones, growth factors and cytokines. Exposure of the feto-placental

endothelium to these molecules may lead to its functional dysregulation, and thus, account for some of the changes observed in fetal growth reflected by many pregnancy pathologies, including GDM (Wadsack et al., 2012). GDM and feto-placental dysfunction are associated by reduced insulin sensitivity and by diminished feto-placental endothelial responsiveness to insulin. Diet or insulin treatment of women with GDM are proved to be effective in normalizing glycemic levels at pregnancy term. Nevertheless, feto-placental endothelial distress remains evident (Sobrevia et al., 2015).

Epigenetics & GDM

The developmental programming hypothesis suggests that the intra uterine environment pre-sets the offspring's phenotype in long term. Therefore, GDM is associated with increased risk for obesity and developing diabetes and cardiovascular diseases in the offspring. One of the mechanisms proposed to explain this *in utero* programming is DNA methylation (Lehnen et al., 2013, Mathew and Ayyar, 2012; Vrachnis et al., 2012).

DNA methylation associates with transcriptional repression mainly through the addition of a methyl group within gene promoters by a covalent modification of cytosine residues catalysed by a group of enzymes called DNA methyltransferases (DNMT); and by forming compact chromatin structures, such as heterochromatin (Pal and Tyler 2016; Lee and Kong 2016). DNMT activity is crucial for gene expression control, for instance, overexpression and deficiency of DNMT1 are shown to be embryonic lethal, and DNMT1 deletion causes genome-wide hypomethylation, whereas DNMT1 overexpression causes genome-wide hypermethylation (Dunn et al., 2015).

Furthermore, the endothelium of the feto-placental vasculature in GDM may be affected by hyperglycaemia and by the pro-inflammatory environment that GDM causes. Preliminary data generated in our laboratory demonstrated that feto-placental arterial endothelial cells isolated from human placentas after healthy pregnancies and after pregnancies complicated by GDM differ in their function, i.e. in their proliferation capacity and angiogenic potential. Therefore, whole genome expression analysis (Affymetrix 1.0 ST gene arrays) in parallel with global scale

DNA methylation analysis (Ilumina Infinium 450K arrays) were employed previously in our lab to identify genes that have altered expression and concomitantly altered DNA methylation. One of the genes identified by these analyses was the gene encoding versican (*VCAN*), which was found hypomethylated and higher expressed in GDM derived cells.

Extracellular matrix proteins & GDM

The placenta is a fast developing and growing organ with various remodeling processes taking place and the ECM plays an important role herein. The ECM is required for many specialized cell functions and is composed by several combinations of molecules and polysaccharides such as collagens, elastin, glycosaminoglycans (GAGs), and proteoglycans (PG) (Giachini et al., 2008).

Versican is an ECM molecule and member of the large aggregating chondroitin sulphate proteoglycan family. In physiological conditions versican levels are low, whereas it increases in several pathologies. Versican structure is composed of an N-terminal G1 domain, a GAG attachment region, and a C-terminal G3 domain. The G3 domain contains two epidermal growth factor (EGF)-like repeats, a lectin-like motif, and a complement binding protein (CBP)-like motif. At least 4 different versican isoforms are generated by alternative splicing (V0-V3), which differ in their glycosaminoglycan region: the central domain of versican V0 (373kDa) contains both the GAG-α and GAG-β domains. The V1 isoform (265kDa) contains the GAG-β domain, V2 (182kDa) the GAG-α domain, and V3 (74kDa) does not have any GAG attachment domains (**Figure 2**) (Wight, 2002; Wight et al., 2014).

Forms of versican containing GAG domains (V0, V1 and V2) are negatively charged and thus, attract H_2O molecules, contributing to the viscoelasticity of the pericellular microenvironment. Versican is known to associate with a number of molecules in the ECM including hyaluronan, tenascin, fibronectin, CD44 and L-selectin, fibrillin1, integrin, and link protein (Wu et al., 2005), influencing cells to proliferate, migrate, adhere and assemble within the ECM. Therefore, the study of the ECM and in particular of versican could help to elucidate mechanisms underlying changes in endothelial function observed in GDM.

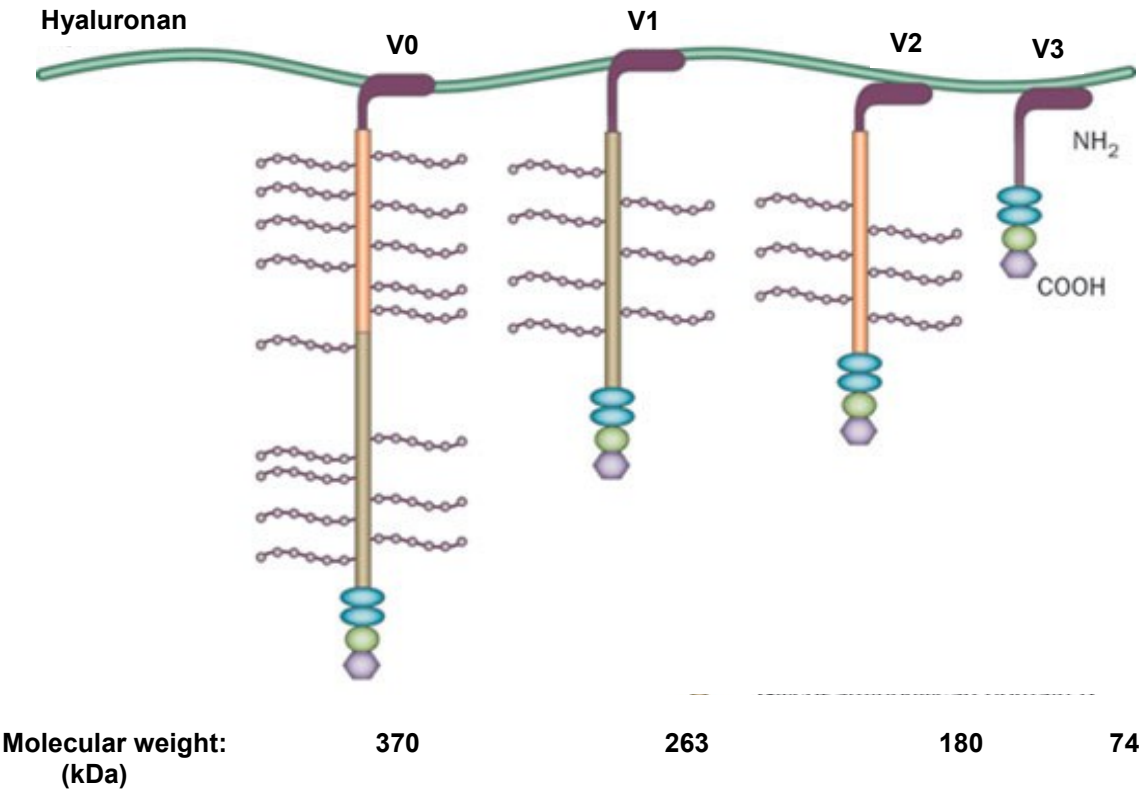

Figure 2. **Structure of versican isoforms.**

Illustration of versican isoforms and their molecular weight. Modified from 'Proteoglycans in prostate cancer' (Edwards, 2012).

Hypothesis & Objectives

Hypothesis:

'Human placental arterial endothelial cells of healthy and GDM pregnancies differ in their phenotype as a result of epigenetic modifications caused by the low-grade pro-inflammatory environment of GDM'.

Objectives:

Identification of particular changes in the epigenome (methylome) of human placental endothelial cells of pregnancies associated with the pro-inflammatory environment of GDM revealed potential targets to be evaluated. Hence, the objectives of this study were:

1. Determine if DNA methylation differences between control and GDM arterial endothelial cells result in transcript and protein changes.

2. Identify the pro-inflammatory components of the diabetic intrauterine environment that lead to these methylation changes.

Materials & Methods

Ethics statement

This study was approved by the Ethical Committee of the Medical University of Graz and informed consent of all patients was obtained. Clinical characteristics of patients were collected on an anonymous basis after coding the patients' names. Summary of clinical characteristics of primary cells separated according to the experiments they were used for are presented in **Table 4**.

Screening for gestational diabetes mellitus

Oral glucose tolerance test (oGTT) is routinely performed between the 24th and the 28th weeks of gestation in our institution. After ingesting 75g of glucose, glycaemic levels in venous plasma were measured. Women were diagnosed for GDM if one measurement was above the defined maximum levels of normal glucose tolerance (fasting glycaemia <5.1mM; 1-hour glucose level <10.0mM; 2-hours glucose level <8.5mM). In case of one pathological value, women received nutritional counselling and were instructed to self-monitor their glucose levels. Insulin therapy was initiated when blood glucose levels failed to be maintained in the normal range (fasting glycaemia <95mg/dl and 1 hour after meals <140mg/dl).

Statistical analysis

Data were analysed using GraphPad Prism Software Version 5.01. Data were expressed as mean ± SEM or minimum and maximum. Student's t test was applied after testing for normal distribution (Kolmogorov-Smirnov test). For multivariable data, ANOVA analysis was performed. p-values below 0.05 were considered statistically significant.

Collection of human cord blood serum

Arterial and venous umbilical cord blood was collected after healthy pregnancies and pregnancies complicated with GDM. Blood was obtained by inserting a syringe into the vessels at delivery. Blood samples were centrifuged at 3500*g* for 15 minutes to obtain the serum. Cord blood serum from arteries and veins of the same patient were pooled on a 1:1 ratio for this study. Aliquots were stored at -80°C until further analysis.

Culture of human first trimester trophoblast

Human first trimester trophoblasts were isolated from first trimester placentas (7 to 10 weeks of gestation). Tissue was washed with cold Hank's Balanced Salt Solution (HBSS) buffer and villi were isolated and digested with Dispase/Dnase (Gibco, Thermo Fisher) and Trypsin (Gibco, Thermo Fisher). Cells were centrifuged in a Percoll gradient (Gibco, Thermo Fisher) and incubated with antibodies against CD-90 and CD-45 (DAKO Denmark A/S) in order to remove fibroblast and common leukocyte-antigen expressing cells. Characterization was performed as previously described (Loegl et al., 2016). Cells were cultured in Ham's F12 medium with L-Glutamine (Gibco, Thermo Fisher) supplemented with 10% fetal calf serum (FCS, HyClone, GE Healthcare) and penicillin/streptomycin (Gibco, Thermo Fisher).

Culture of human first trimester trophoblast cell line (ACH-3P)

A cell line of first trimester trophoblast (ACH-3P) previously stablished in our lab (Hiden et al., 2007) was used. Cells were cultured in Ham's F12 medium containing L-Glutamine (Gibco, Thermo Fisher) supplemented with 10% fetal calf serum (FCS, HyClone, GE Healthcare) and penicillin/streptomycin (Gibco, Thermo Fisher).

Culture of human term placental arterial endothelial cells

Primary arterial endothelial cells (AEC) from human term placentas after healthy pregnancies (control) and pregnancies complicated by GDM were isolated using a standard protocol previously described (Lang et al., 2008). AEC were characterized by immunocytochemistry and internalization of acetylated low-density-lipoprotein (Biomedical Technologies, Stoughton MA). AEC were cultured on 1% gelatine pre-coated T75 flasks using Endothelial Basal Medium (EBM) supplemented with the EGM-MV BulletKit (Lonza, Belgium). For cell expansion, cells were maintained at 12% O_2, 37°C until confluence and then detached with trypsin/EDTA (Gibco, UK) and counted by using the cell counter and analyser system CASY 1® (Schärfe System GmbH, Reutlingen, Germany). 800000 viable cells were seeded on a T75 flask and cultured at 21% O_2, 37°C for 48 hours.

Culture of human term placental arterial smooth muscle cells

After isolating the endothelial cell layer of the arteries, arteries were rinsed with HBSS, cut longitudinally and dissected into small pieces (3-5mm). Explants were placed with the lumens down in 10cm^2 Petri dishes and cultured with DMEM supplemented with 10% fetal bovine serum (FBS, Lonza, Belgium) at 37°C, 5% CO_2. After 10-12 days, cells were transferred to T25 or T75 flasks and cultured with SmBM supplemented with SmGM-2 BulletKit (Lonza, Belgium). Characterization was performed by immunocytochemistry. After transference to T25/T75 flasks, supernatant was collected every 2 days and after confluency, total RNA was isolated.

Culture of human term trophoblasts

Primary villous trophoblasts were isolated from term placentas after healthy and GDM pregnancies. Villous tissue was minced and digested with an enzymatic solution containing trypsin (Gibco, UK), dispase (Roche, Germany) and DNase (Sigma, USA). Cells were centrifuged in a Percoll gradient (Gibco, Thermo Fisher) and negative selection with mouse monoclonal MCA-81-conjugated magnetic beads (Sigma, USA) was assessed in order to obtain pure cultures of villous

trophoblast. Cells were cultured in DMEM (Gibco, UK) supplemented with 10% FBS (Lonza, Belgium), HEPES (20mM, pH 7.4, Sigma) and penicillin/streptomycin (Sigma). Phenotypic and functional characterization was performed as previously described (Loegl et al, 2016).

Culture of human umbilical vein endothelial cells (HUVEC)

Human umbilical vein endothelial cells (HUVEC) were purchased from Cambrex (New Jersey, USA). HUVEC were cultured in Endothelial Cell Basal Medium (EBM, Lonza, Belgium) supplemented with 10% fetal bovine serum (Lonza, Belgium) and penicillin/streptomycin (Gibco, Thermo Fisher). Cells were used until passage 7.

Determination of intracellular nitric oxide bioavailability

Evaluation of transient intracellular nitric oxide (NO) levels was performed using the fluorescent probe 4-amino-5-methylamino-2′,7′-difluorofluorescein (DAF, Sigma) as previously described (Searle et al., 2011). AEC from control and GDM placentas were seeded in 96-well black plates (20000 cells/well) in 100µL EBM with supplements, and maintained overnight at 21% O_2 and 37°C. AEC were deprived from serum for 5 hours in order to decrease cell metabolism to basal levels. Then cells were incubated with L-arginine (100µM) and the fluorescent probe DAF-FM diacetate (2µM) for 30 minutes, following stimulation with insulin (10nM) or HBSS for 15 minutes. Fluorescence intensity was determined using a fluorometer (FLUOstar OPTIMA; BMG Labtech) with 485nm excitation and 520nm emission wavelengths.

Enzyme-linked immunosorbent assay (ELISA)

Endothelial cells were cultured (800000 cells per T75 flasks) at 21% O_2, 37°C for 48 hours, after collecting the supernatant, cells were washed twice with cold phosphate buffer saline (PBS), detached with trypsin/EDTA and washed twice. Cell pellet was re-suspended on 200µl of PBS and sonicated with the UP100H-Compact Ultrasonic

Laboratory Device (Hielscher, Germany), followed by 15 minutes of cold-centrifugation (4°C) at 13000rpm in order to remove cell debris. Collected supernatant was concentrated using the Amicon Ultra-4 Centrifugal Filter Unit with Ultracel-10 membrane (Merck Millipore, Ireland).

Intracellular protein levels were measured with ELISA kits for Cyclin D2, Cyclin-dependent kinase 4 (CDK4), fibrillin1, TGFβI and versican (USCN, Life Science Inc.), respectively, following the instructions of the manufacturer. Levels of versican and TGFβI in conditioned media were also measured with the ELISA kit. Obtained values were normalized with the total protein concentration measured by the Bicinchoninic acid assay (BCA) method using the Pierce BCA Protein Assay Kit (Pierce, Thermo Scientific).

Immunoblot

Protein levels were determined by immunoblot. Protein isolation was performed depending on the nature of the molecule studied. 800000 cells were cultured on T75 flasks at 21% O_2, 37°C for 48 hours. Cells were washed twice with HBSS and protein was extracted with RIPA buffer containing protease inhibitors (Complete Protease Inhibitor Cocktail Tablets, Roche). Cell lysate (10µg of total protein) were applied to a gradient 4-20% SDS-PAGE, and transferred by electrophoresis to 0.2µm nitrocellulose membranes (Trans-Blot Turbo Mini Nitrocellulose Transfer Membrane, BioRad) using the Trans-Blot Turbo Transfer System (BioRad). Proteins of interest were detected with the primary and secondary antibodies according to the **Table 1**. Between each antibody incubation, nitrocellulose membranes were washed for one hour with tris-borate-EDTA buffer containing 1% tween (TBE-tween) buffer. Signals were detected using the SuperSignal West Pico or Femto Chemiluminescent Substrate (Pierce, Thermo Scientific, Rockford, IL, USA).

Immunoblot for versican

Cells were cultured (800000 cells /T75 flask) for 48 hours. After washing cells with PBS, protein was extracted with 8M Urea solution (containing 8M urea, 2mM EDTA,

50mM Tris Base, 0.5% Triton X-100, 0.25M NaCl, pH 7.5) and proteinase inhibitors (Complete Protease Inhibitor Cocktail Tablets, Roche). Cell lysate and supernatants were separately passed through DEAE-sephacel (Sigma Aldrich) columns previously equilibrated with 8M Urea solution. Concentrated proteoglycans were ethanol precipitated and digested with chondroitinase ABC (Sigma Aldrich). Digested proteoglycans were applied to a gradient 4-20% SDS-PAGE, and treated as described previously for immunoblot. Primary and secondary antibodies were used according to **Table 2**.

Immunohistochemistry

Placental tissue samples from healthy (n=4) and GDM pregnancies (n=4) were fixed and paraffin embedded using the HOPE fixation technique (Innovative Diagnostik Systeme, Hamburg, Germany) as previously described (Blaschitz et al., 2008). Sections of Placental tissue (5µm) were mounted on Superfrost Plus slides (Menzel/Thermo Fisher Scientific), deparaffinized in xylene and rehydrated in a graded series of ethanol. Sections were immunostained using the UltraVision Large Volume Detection System HRP Polymer Kit (Thermo Scientific, Rockford, IL, USA) according to the manufacturer's protocol. After blocking for 10 minutes, slides were washed 3 times with Tris-buffered saline (TBS), and background blocking was performed using Ultra Vision Protein Block for 5 minutes. Incubation with rabbit monoclonal anti-ICAM1 antibody (ab109361, Abcam, 1:250) diluted in Antibody Diluent (Dako Denmark A/S) was performed at room temperature for 45 minutes. Slides were washed and detection assessed by incubation with the anti-mouse/rabbit UltraVision HRP-labeled polymer system and 3-amino-9-ethylcarbacole (AEC, Thermo Scientific), according to the manufacturer's instructions. Hemalaun staining was assessed to detect cell nuclei. For negative controls, slides were incubated with a polyclonal rabbit IgG antibody (negative control for rabbit IgG Ab-1, Thermo Scientific, 2mg/ml).

CD11 and CD18 staining was performed on standard formalin fixed paraffin embedded term placenta sections (5µm) as previously described (Diaz-Perez et al., 2016). Sections were stained using monoclonal anti-CD11 antibody (clone EP1345Y, Merck Millipore, 1:50) and polyclonal anti-CD18 (NBP1-88128, Novus,

1:10). Images were acquired using a Zeiss Axiophot microscope equipped with an AxioCamHRc digital camera.

Immunofluorescent staining

Cryosections (5µm) of human term placental samples were mounted on microslides (Assistent, Karl Hecht AG, Sondheim, Germany). Endothelial cells were grown on gelatin-coated glass chamber slides (Lab-Tek II, Nalgene Nunc International, Naperville, IL, USA) and washed with PBS before harvest. Cryosections and chamber slides were air-dried overnight and stored frozen. Prior to immunostaining, tissue and cells were fixed in acetone for 4 minutes.

For immunofluorescence staining, primary antibodies for versican V0 (polyclonal goat anti human, R&D Systems, 5µg/ml), CD34 class II (mouse IgG1, clone QBEnd-10, DAKO Denmark A/S, 5µg/ml,) and von Willebrand factor (polyclonal rabbit anti human, DAKO Denmark A/S, 0.7 µg/ml) were applied for 30 minutes at room temperature. Following secondary antibodies were used: DyLight550 (donkey anti goat, ThermoFisher Scientific, 5µg/ml), Alexa Fluor 488 (goat anti rabbit, Life Technologies, Invitrogen, 5µg/ml) and FITC (goat anti mouse, BD Pharmingen, 10µg/ml). Slides were counterstained with DAPI (4',6 diamidino-2-phenylindole, Invitrogen, 2.5µg/ml), mounted with ProLong Gold antifade reagent (Invitrogen) and analyzed by fluorescent microscopy using a Leica DM6000B microscope connected to an Olympus DP72 digital camera (Olympus, Austria).

Proteoglycan synthesis

Incubation of cells with [^{35}S]-sulphate (40µCi) was performed 24 hours after seeding the cells with a density of 1x10^5 cells/cm^2. After 24 hours, supernatant was collected. Cells were washed with PBS and protein was extracted with 8M Urea solution containing proteinase inhibitors.

In order to remove excess unincorporated [^{35}S]-sulfate and to isolate [^{35}S]-proteoglycans, samples were applied through DEAE-sephacel (Sigma Aldrich)

columns in 8M Urea eluting solution (containing 8M Urea, 2mM EDTA, 50mM Tris Base, 0.5% Triton X-100, 2M NaCl, pH 7.5).

Samples were applied to a large SDS-Page gel (3.5% stack/4-12% resolving gel, 18x16cm) at reducing condition overnight at 5-6 mA and transferred to a 0.2µm nitrocellulose membrane (Biorad Semidry Electro-transfer apparatus) for 3 hours at 20V (397mA). Auto-radiographic films were exposed to the membrane for 2 days.

For determination of [^{35}S]-proteoglycans levels in aliquots of cell and medium fractions were counted for radioactivity. And aliquots of cell fractions were used for protein determination with the BCA method.

Portions of 100µl of radioactive solution were applied in duplicate to strips (4cm x 26cm) of Whatman 3MM filter paper at intervals of 4cm. Strips were mounted vertically in steel racks carrying eight strips each (LKB, Stockholm, Sweden). The dried strips were washed 5 times for 30 minutes each using 1000ml of 1% cetylpyridinium chloride prepared in 0.3M NaCl. After another drying step, squares (4cm x 4cm) with the applied samples were cut and transferred to scintillation vials. After the addition of 1ml water and 10ml Insta-Gel, the samples were left to equilibrate for 1 hour. Scintillation liquid was added to count radioactivity using a Beckman Model LS250 liquid scintillation counter (Packard Instruments, Warrenville, Ill., U.S.A.). Values of approximately 40 disintegrations per minute (CPM) were considered as background levels.

Table 1. Antibodies and concentrations used for detection of cell cycle proteins by immunoblot.

Antibody against	Company	MW (kDa)	Host specie	1st ab dilution	2ary ab dilution	Working Solution
14.3.3 η	Cell signaling	28	Rabbit	1:2000	1:4000	5% BSA in TBE-tween
CDC47/mcm7	Cell signaling	80	Rabbit	1:1000	1:3000	5% BSA in TBE-tween
CDK5	Cell signaling	35	Rabbit	1:2000	1:4000	5% BSA in TBE-tween
CUL1	Abgent	90	Rabbit	1:2000	1:4000	5% Milk in TBE-tween
CUL3	Abgent	82-90	Rabbit	1:10000	1:6000	5% Milk in TBE-tween
GAPDH	Novus	36	Mouse	1:20000	1:6000	5% Milk in TBE-tween
p27/kip1	Cell signaling	27	Mouse	1:1000	1:3000	5% Milk in TBE-tween
Rabbit	Bio-Rad	N/A	Goat	N/A	N/A	N/A
Mouse	Bio-Rad	N/A	Goat	N/A	N/A	N/A

Table 2. Antibodies and concentrations used for versican detection by immunoblot.

Antibody against	Company	MW (kDa)	Host specie	1st ab dilution	2ary ab dilution	Working Solution
GAPDH	Novus	36	Mouse	1:20000	1:6000	5% milk in TBE-tween
Versican V0, V1 Neo (DPEAAE fragments)	Thermo Fisher Scientific Pierce	70	Rabbit	1:3000	1:6000	5% milk in TBE-tween
Versican (V0)	R&D	373	Goat	1:6000	1:6000	2% BSA in TBS-tween
Goat	Bio-Rad	N/A	Rabbit	N/A	N/A	N/A
Rabbit	Bio-Rad	N/A	Goat	N/A	N/A	N/A
Mouse	Bio-Rad	N/A	Goat	N/A	N/A	N/A

RNA isolation and RT-qPCR

After culture, cells were washed twice with HBSS and total RNA was isolated and purified with the RNeasy Mini Kit (Qiagen, Hilden, Germany). The quality and integrity of the RNA was determined by the ratio of spectrophotometric absorbance 260nm/280nm measured with the Scandrop 250 (Analytick Jena AG, Germany).

The cDNA was synthesized from 1000ng of total RNA according to the manufacturer's instructions (SuperScript II Reverse Transcriptase protocol from Invitrogen, USA). Total RNA pools of fetal brain, kidney, thymus, heart and spleen were purchased by Clontech (CA, USA).

Real-time PCR was performed using TaqMan gene expression assays from Applied Biosystems (CA, USA) for the respective genes (**Table 3**) using 3.125 ng/µl of cDNA on a total reaction volume of 10µl, and the ABI Prism 5,700 Sequence Detection System. As an internal control hypoxanthine-guanine phosphoribosyltransferase (*HPRT1*) expression was used since it was not influenced by GDM. Data were analyzed according to the 2-ΔΔCt method (Bustin, 2002; Bustin et al., 2005).

Table 3. Genes evaluated and their gene codes.

Gene	TaqMan Primer, gene code
ABR	Hs01077824_m1
ANGPT2	Hs01048042_m1
APEX	Hs00959050_g1
ATR	Hs00992123_m1
CCNC	Hs01029304_m1
CCND2	Hs00153380_m1
CDC14A	Hs00186432_m1
CDC47	Hs00428518_m1
CDK1	Hs00938777_m1
CDK2	Hs01548894_m1
CDK4	Hs01565683_g1
CDK5	*Hs00358991_g1*
CDK8	Hs00176209_m1
CDKN1A	Hs00355782_m1
CDKN1B	*Hs01597588_m1*
CDKN1C	Hs00175938_m1
CHEK1	Hs00967506_m1
CTNNB1	Hs00355049_m1
CUL1	*Hs01117001_m1*
CUL3	*Hs00180183_m1*
DNMT1	Hs00945875_m1
EP300	Hs00914223_m1
E-SELECTIN	Hs00950401_m1
FANCC	Hs00984545_m1
FBN1	Hs00171191_m1

FOXM1	Hs01073586_m1
GADD45A	Hs00169255_m1
GADD45B	Hs04188837_g1
GJA5	Hs00270952_s1
GSK3B	Hs01047719_m1
H19	Hs00262142_g1
HRPT1	Hs02800695_m1
ICAM-1	Hs00164932_m1
IGF1R	Hs00609566_m1
IL-6	Hs00985639_m1
NOS3	*Hs01574665_m1*
NOTCH4	Hs00965889_m1
OCLN	Hs00170162_m1
PXN	Hs01104424_m1
RAD51	Hs00153418_m1
RRM1	Hs01040698_m1
SERPINE1	Hs01126607_g1
TGFB1	Hs00998133_m1
TGFBI	Hs00932747_m1
VCAM1	Hs01003372_m1
VCAN (all isoforms)	Hs00171642_m1
VCAN (V1)	Hs01007944_m1
VCAN (V1, V3)	Hs01007938_m1
VCAN (V2)	Hs01007941_m1
VCAN (V3)	Hs01007938_m1
VCAN (V4)	Hs01007943_m1
YWHAH	Hs00607046_m1

Tube-formation fibrin assay

After confluency, control and GDM AEC were seeded on 3D human fibrin matrices prepared as described (Koolwijk et al., 1996). Following overnight incubation in M199 supplemented with 10% human serum (HS) and 10% new-born calf serum (NBCS, Gibco, ThermoFisher) and 10ng/ml FGF2, cells were stimulated with 25ng/ml vascular endothelial growth factor (VEGF), 10ng/ml tumor necrosis factor-α (TNF-α), 50pg/ml transforming growth factor-β1 (TGFβ1), respectively, and the following combinations of them: VEGF+TGFβ1, VEGF+TNFα and VEGF+TNFα+TGFβ1. All growth factors were purchased from ReliaTech, Wolfenbuttel, Germany. After 48-hours stimulation, cells were stimulated a second time. 72 hours after the second stimulation, cells were washed twice and fixed with a pre-warmed solution of 2% paraformaldehyde and quantification of the length of formed tube-like structures was performed using Optimas 6.5 image analysis software as previously described (Koolwijk et al., 1996).

siRNA transfection on tube-formation assay

Versican effect in tube formation was determined in fibrin matrices. siRNAs against *VCAN* (Hs_VCAN_5 FlexiTube siRNA, cat.no. SI04948587) were purchased from Qiagen and prepared according to manufacturer's instructions. Non-targeting siRNA was purchased from GE Dharmacon (Lafayette, CO). Cells were cultured with supplemented media without antibiotics overnight before transfection with DharmaFECT1 reagent (Dharmacon). All siRNA and DharmaFECT1 were prepared in M199 + 10% HS supplemented with 10ng/ml FGF2. Cells were seeded onto fibrin matrices and after cell attachment, transfection medium was added. 20 hours after transfection, medium was replaced by stimulation-medium containing VEGF and TNFα. Since smooth muscle cells (SMC) are reported to produce and secrete versican (Wight and Merrilees, 2004), cells were stimulated with recombinant versican (Novus) or supernatant of cultured smooth muscle cells isolated from human placentas after healthy (control SMC) or GDM pregnancies (GDM SMC). Transfection efficiency was evaluated by RT-qPCR. Stimulation was repeated 48h after the first stimulation and 24 hours after, experiments were finalized by fixation with 2% PFA. Length of formed tube-like structures was quantified as previously described (Koolwijk et al., 1996).

Results

1. Determine if DNA methylation differences between control and GDM arterial endothelial cells result in transcript and protein changes.

Transcript changes: selection of target genes

Based on preliminary data, target genes were selected to be evaluated by RT-qPCR using specific TaqMan Primers. Gene expression and p-value between AEC isolated after control and GDM pregnancies are summarized in **Table 5**. Expression of *VCAN*, *TGFBI*, *FBN1*, *IGF1R*, *CCND2*, *EP300*, *GADD45B*, *CDK2*, *IL6*, *FANCC*, *DNMT1* and *APEX* ($p<0.05$) was found to be increased in GDM AEC compared to control AEC.

Table 4. **Clinical characteristics of patients.**

Assay	Number of subjects	Gestational age (weeks)	CRP (nmol/l)	Placental weight (g)	Fetal ponderal index (kg/m^3)	BMI before pregnancy (kg/m^2)	BMI before delivery (kg/m^2)
RTqPCR	Control (n=23) GDM (n=12)	39.5±1.3 38.7±0.9	5.4±4.5 6.4±5.4	632.0±196.6 680.0±148.5	26.1±2.9 26.3±2.4	24.2±4.7 27.3±7.2	31.3±6.7 31.6±6.9
Immunoblot	Control (n=22) GDM (n=11)	39.3±1.6 38.5±1.1	5.2±2.9 5.1±3.8	627.7±173.8 725.0±377.1	26.6±2.9 26.4±2.3	22.9±1.9 26.6±6.6	27.0±3.0 31.6±6.7
ELISA	Control (n=12) GDM (n=9)	39.2±1.6 38.3±1.3	4.2±1.8 5.2±4.0	594.2±102.9 725.0±198.2	25.7±2.5 26.1±2.1	22.6±2.6 26.4±6.9	33.3±8.3 31.2±7.2
Angiogenesis	Control (n=9) GDM (n=6)	39.2±1.0 38.9±1.2	5.0±3.2 6.2±6.1	558.8±102.3 632.5±80.2	26.1±2.1 26.4±2.0	23.2±2.7 28.6±7.2	33.6±5.6 34.7±3.0
NO bioavailability	Control (n=8) GDM (n=6)	39.4±1.6 38.8±0.8	5.7±3.1 8.1±5.9	556.3±95.0 610.0±160.2	26.3±4.1 24.0±0.4	22.8±2.4 28.8±9.4	26.3±2.2 32.5±8.5

Reference range for C-reactive protein (CRP)= 0.76-28.5 (nmol/l). BMI categories (kg/m^2): underweight ≤18.5, normal weight = 18.5–24.9, overweight = 25–29.9 and obesity ≥ 30.

Table 5. RT-qPCR for selecting target genes.

Cells were cultured with complete media for 48 hours at 21% O_2 & 37°C, gene expression was normalized to *HPRT1*.

Gene	Fold change Control vs. GDM AEC	p-value
VCAN	41.06	0.0001
TGFB1	6.48	0.0001
FBN1	5.58	0.0001
IGF1R	5.53	0.002
EP300	2.95	0.002
FANCC	1.83	0.003
IL-6	2.70	0.007
APEX	1.81	0.016
GADD45B	2.52	0.025
DNMT1	1.38	0.026
CCND2	3.39	0.028
CDK2	1.86	0.044
NOS3	2.00	0.052
CHEK1	2.33	0.051
GADD45A	1.75	0.058
CDK4	1.41	0.061
NOTCH4	1.99	0.105
GJA5	2.45	0.128
RRM1	1.62	0.168
SERPINE1	1.50	0.198
RAD51	1.54	0.258
OCLN	0.71	0.289
CDC47	1.17	0.326

FOXM1	0.93	0.491
PXN	0.75	0.568
VCAM1	1.60	0.678
E-SELECTIN	1.25	0.707
ATR	0.87	0.747
ANGPT2	1.08	0.773
ABR	0.94	0.887

Versican evaluation

Versican exhibited the highest fold change (a 41-fold increase) of gene expression between control and GDM AEC. Therefore, further experiments focused on versican. 4 isoforms of versican are described (V0, V1, V2 and V3), thus, RT-qPCR were performed with specific TaqMan primers for V0, V2, V3 and V0/V1. V0 was 300-fold upregulated in AEC from GDM pregnancies ($p<0.01$), V0/V1 was 308-fold upregulated ($p<0.001$), V2 was 43-fold upregulated although it was not significant, and V3 was only detected in GDM AEC.

To confirm differences in versican also on protein level ELISAs were performed. ELISA for total versican, i.e. all isoforms, showed no difference between control and GDM AEC (**Figure 3a**), however, levels of total versican in supernatant of cultured GDM AEC were decreased by 48% compared to control ($p<0.05$) (**Figure 3b**). Furthermore, evaluation of versican V0 by an ELISA specific only for V0 revealed higher levels in cell lysate of GDM compared to control AEC ($p<0.01$) (**Figure 3c**), but no difference in supernatant of cultured cells (**Figure 3d**).

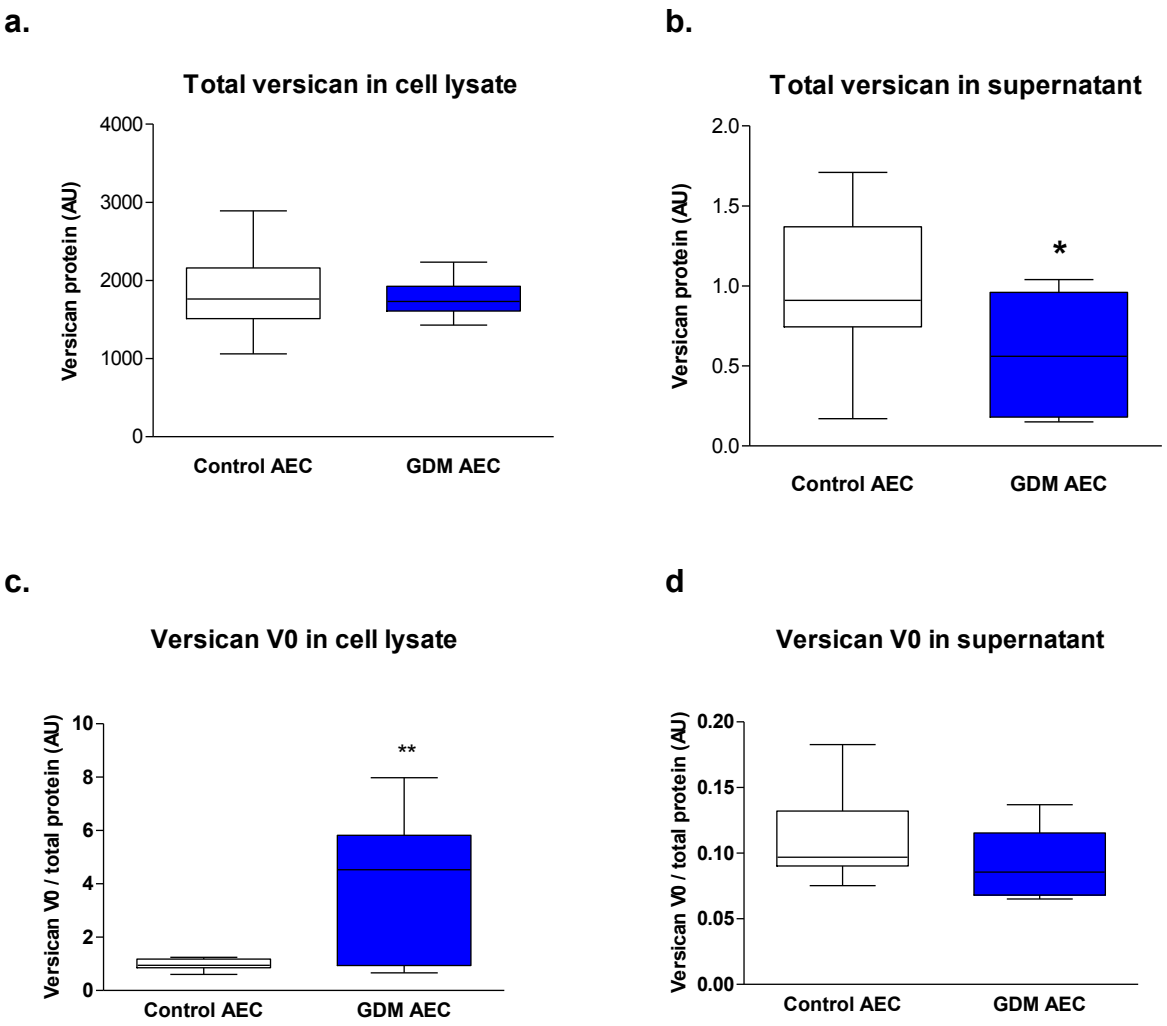

Figure 3. Protein levels of total versican and V0 as determined by ELISA.

a. Levels of total versican determined by ELISA, using 5µg of total protein ($n_{control\ AEC}$ = 9; $n_{GDM\ AEC}$ = 9). **b.** Total versican levels in supernatant of cultured cells, values were normalized to the total protein content ($n_{control\ AEC}$ = 9; $n_{GDM\ AEC}$ = 7). **c.** Protein levels of versican V0 in total cell lysate normalized to total protein content ($n_{control\ AEC}$ = 8; $n_{GDM\ AEC}$ = 9). **d.** Protein levels of versican in supernatant of cultured cells, normalized to the total protein content ($n_{control\ AEC}$ = 7; $n_{GDM\ AEC}$ = 5). *p<0.05; **p<0.01

Proteoglycan (PG) synthesis showed higher levels of PG in the supernatant of cultured cells than in the cell layer extract by SDS-PAGE (**Figure 4a**) and by radioactive counting after [^{35}S]-sulphate incorporation (**Figure 4b**), indicating that most proteoglycans are secreted by AEC.

a.

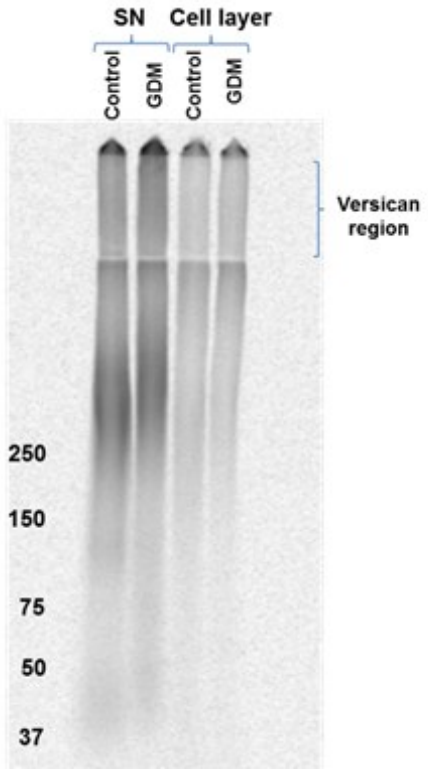

b.

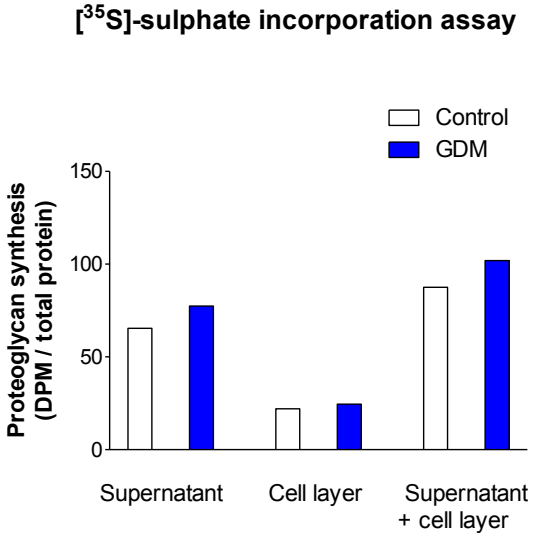

Figure 4. Proteoglycan synthesis in human placental arterial endothelial cells.
Control and GDM AEC were radiolabeled for 24 hours with 40µCi [^{35}S]-sulphate. Protein of supernatant and cell layer were isolated and passed through DEAE columns. PG synthesis was evaluated by SDS-PAGE and membrane was developed by autoradiography **(a)**. Portions of the radioactive solutions were applied to strips of Whatman 3MM filter paper, and radioactivity of the dried strips was counted **(b)** ($n_{control\ AEC} = 1$; $n_{GDM\ AEC} = 1$).

Furthermore, immunofluorescence staining showed no versican V0 expression in cultured control AEC (**Figure 5a**) neither in GDM AEC (**Figure 5b**), while cultured fibroblasts isolated from control placental arteries exhibited strong versican V0 signal (**Figure 5c**).

Since versican V0 was not detected in cultured AEC by immunostaining, immunoblot for versican V0/V1 was assessed. Samples were run through DEAE-Sephacel mini columns (ion exchange) prior to precipitation and chondroitinase digestion. SDS-PAGE was performed using a 3.5% stacking/4-12% gradient big gel (18x16cm) to maximize the separation. No signal was detected in the cell layer, nor in supernatant of control AEC. Versican V0/V1 was detected only in one GDM AEC isolation (**Figure 6**).

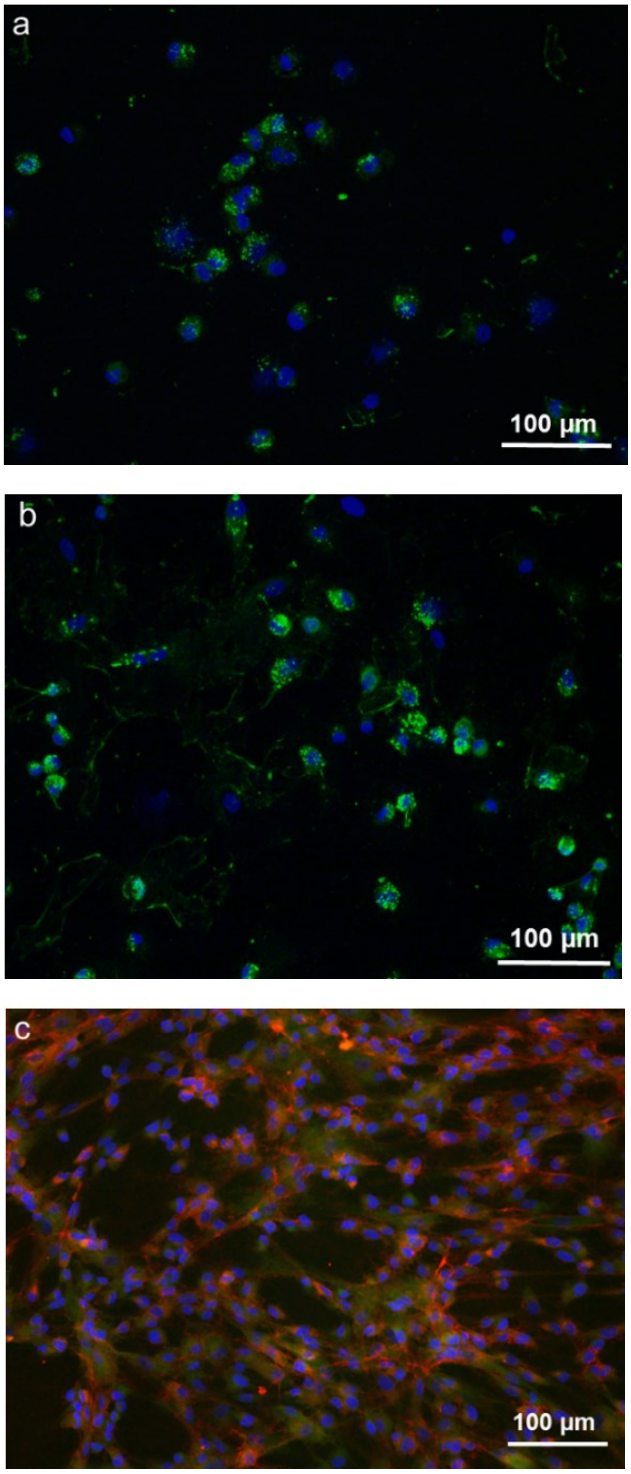

Figure 5. Immunolocalization of versican in human arterial endothelial cells.
AEC from human control (**a**) and GDM placentas (**b**); remained unstained by versican (V0) antibody (absent red staining). von Willebrand factor is shown in green, nuclei in blue. Fibroblasts isolated from human placenta were used as a positive control for versican staining (**c**). Versican V0 is shown in red, CD90 in green and nuclei in blue.

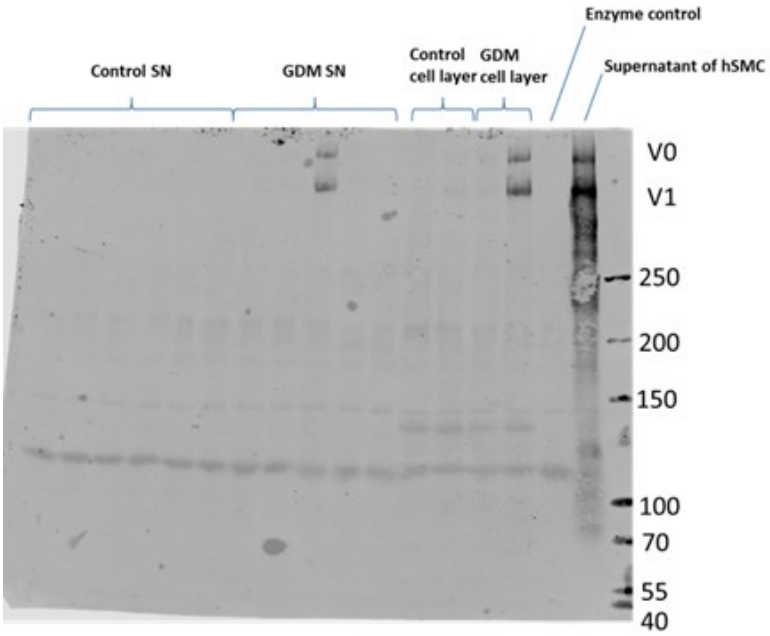

Figure 6. **Versican V0/V1 immunoblot in endothelial cells of human placenta.**
Immunoblot using an antibody which detects versican V0/V1 by binding to the C-terminus of versican, (Seikagaku 2B1) was assessed with supernatant (SN) and cell layer lysate of cultured AEC ($n_{\text{control SN AEC}} = 5$; $n_{\text{GDM SN AEC}} = 5$; $n_{\text{control cell layer AEC}} = 2$; $n_{\text{GDM cell layer AEC}} = 2$).

As immunoblot revealed versican V0/V1 only in one GDM AEC isolation, but also exhibited protein bands between 100 and 200kDa, presence of fragments after proteolytic cleavage of versican were evaluated. Immunoblot revealed similar levels of versican fragments in control and GDM derived AEC (**Figure 7a**). Versican fragments present in the supernatant of AEC were also similar in control and GDM derived cells (**Figure 7b**). Supernatant of cultured cells showed a tendency for decreased versican secretion by GDM derived AEC (**Figure 7c**). No versican was found in cell layer samples (data not shown).

Together with versican, its binding partners fibrillin1 and TGFβI showed differences in gene expression and DNA methylation between control and GDM AEC. RT-qPCR revealed 5.6 fold ($p<0.001$) and 6.5 fold ($p<0.001$) increase in *FBN1* and *TGFβI*, respectively. Therefore, protein levels of fibrillin1 and TGFβI were evaluated by ELISA. Levels of both, fibrillin1 (FC=2.0; $p<0.05$) (**Figure 8a**) and TGFβI were higher in GDM derived AEC (FC=2.7; $p<0.01$) when compared to control AEC (**Figure 8b**). TGFβI levels in supernatant of cultured cells were below the detection limit (data not shown).

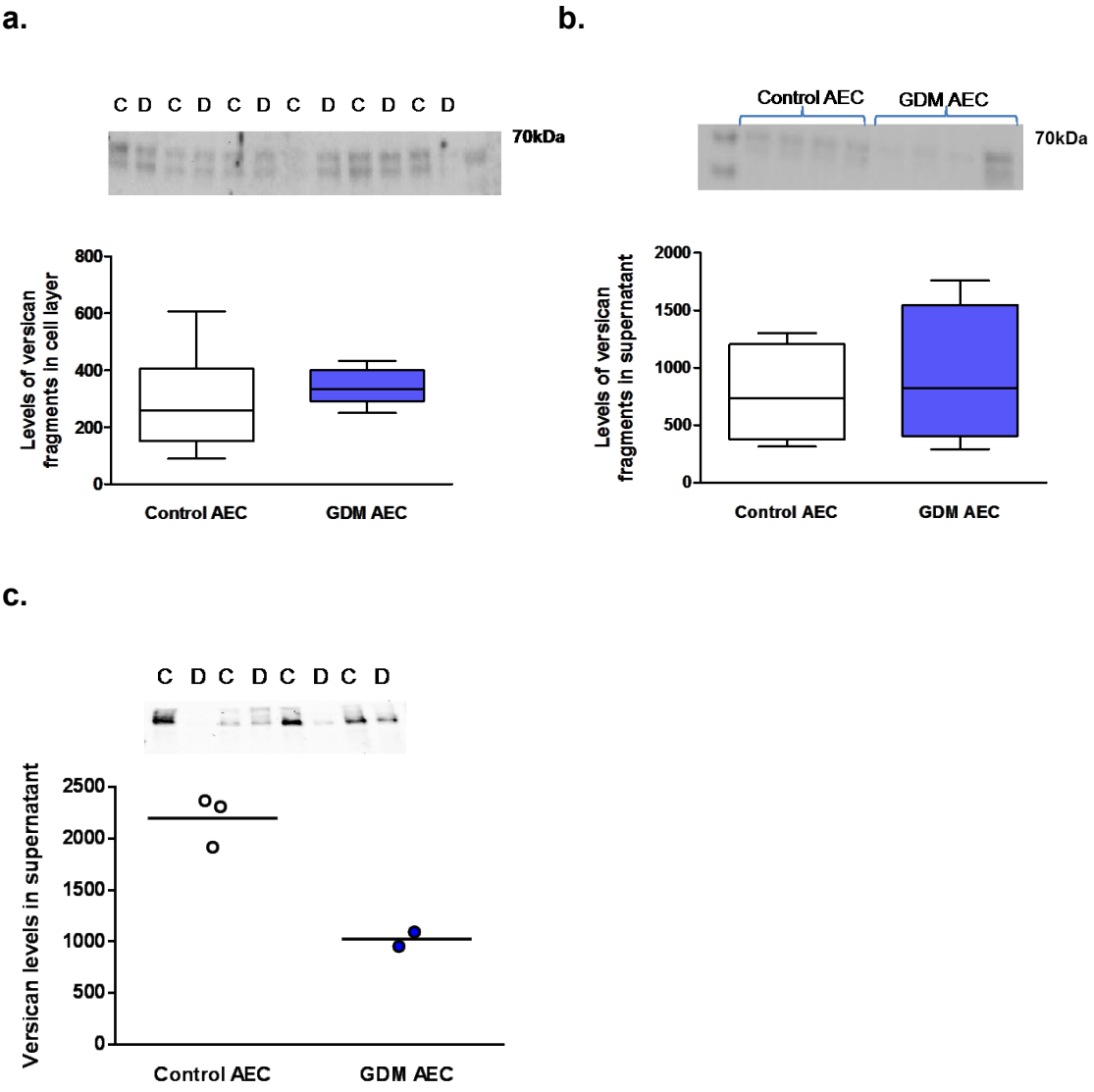

Figure 7. Levels of versican fragments in cell layer and supernatant of cultured human placental arterial endothelial cells.

a. Immunoblot revealed similar levels of versican fragments in control AEC and GDM derived-AEC ($n_{\text{control cell layer AEC}} = 11$; $n_{\text{GDM cell layer AEC}}$). **b.** Fragments of versican in supernatant had similar levels in control and GDM samples ($n_{\text{control SN AEC}} = 4$; $n_{\text{GDM SN AEC}} = 4$). **c.** Supernatant of cultured cells revealed tendency towards decreased versican expression in GDM ($n_{\text{control SN AEC}} = 4$; $n_{\text{GDM SN AEC}} = 4$). There was no versican protein expression in cell layer samples (data not shown). C: control AEC; D: GDM AEC.

a.

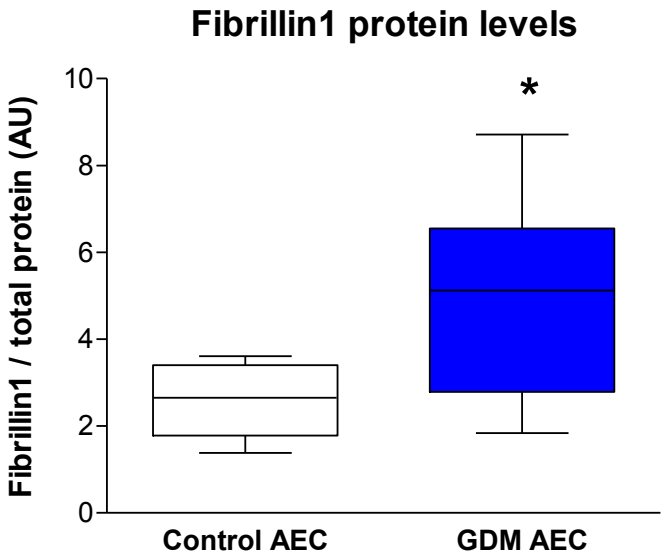

b.

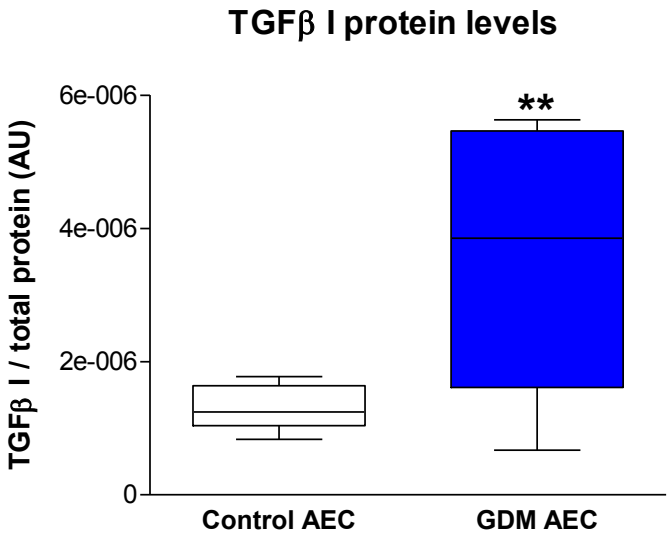

Figure 8. Protein levels of fibrillin1 and TGFβI in human placental arterial endothelial cells.

a. Detection of fibrillin1 in control and GDM AEC by ELISA ($n_{control\ AEC} = 7$; $n_{GDM\ AEC} = 9$). **b.** Protein levels of TGFβI in control and GDM AEC determined by ELISA ($n_{control\ AEC} = 8$; $n_{GDM\ AEC} = 8$). * $p<0.05$; ** $p<0.01$

Furthermore, versican V0/V1 in human placental tissue was evaluated. Lyophilized/desalted samples were concentrated through DEAE Sephacel mini columns prior to precipitation and chondroitinase digestion. And SDS-PAGE was performed using a 3.5% stacking/4-12% gradient big gel (18 x 16cm). Immunoblot for versican in control and GDM placentas revealed a tendency of increased versican in GDM placenta (**Figure 9**).

Immunostainings for versican (V0) in placental tissue were performed. Large blood vessels (arteries and veins) revealed stronger signal of V0 in control placental tissue (n=1) compared to GDM placental tissue (n=1), while versican signal was stronger in villous stroma of GDM vs. control placental tissue (**Figure 10a** and **10b**). Moreover, V0 was not localized in endothelial cells (**Figure 10c**, **10d**, **10e** and **10f**), but in sub-endothelial layers instead.

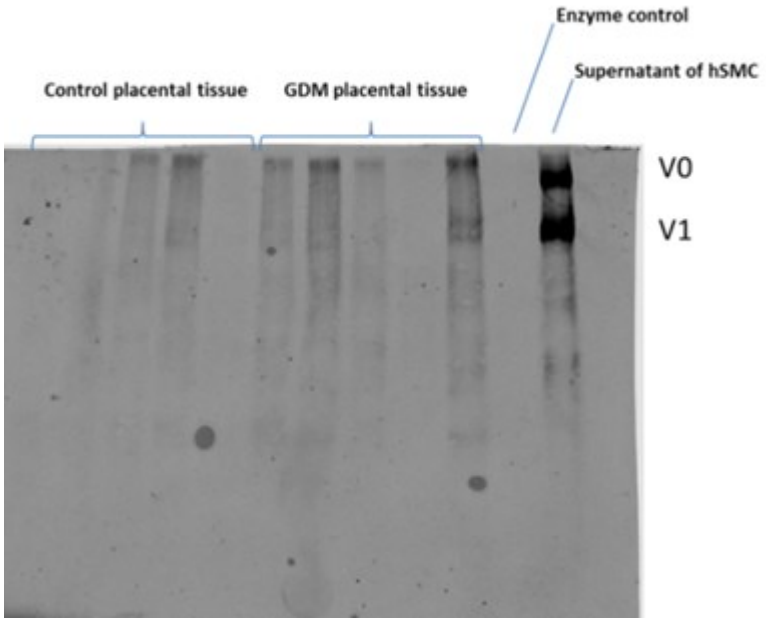

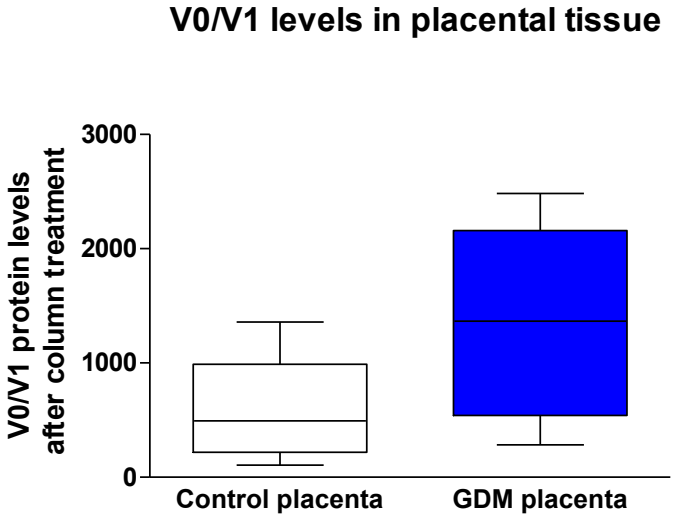

Figure 9. **Immunoblot for versican V0/V1 in human placental tissue.**

Detection of versican in control and GDM placental tissue by immunoblot ($n_{control\ placenta} = 5$; $n_{GDM\ placenta} = 5$) and its quantification.

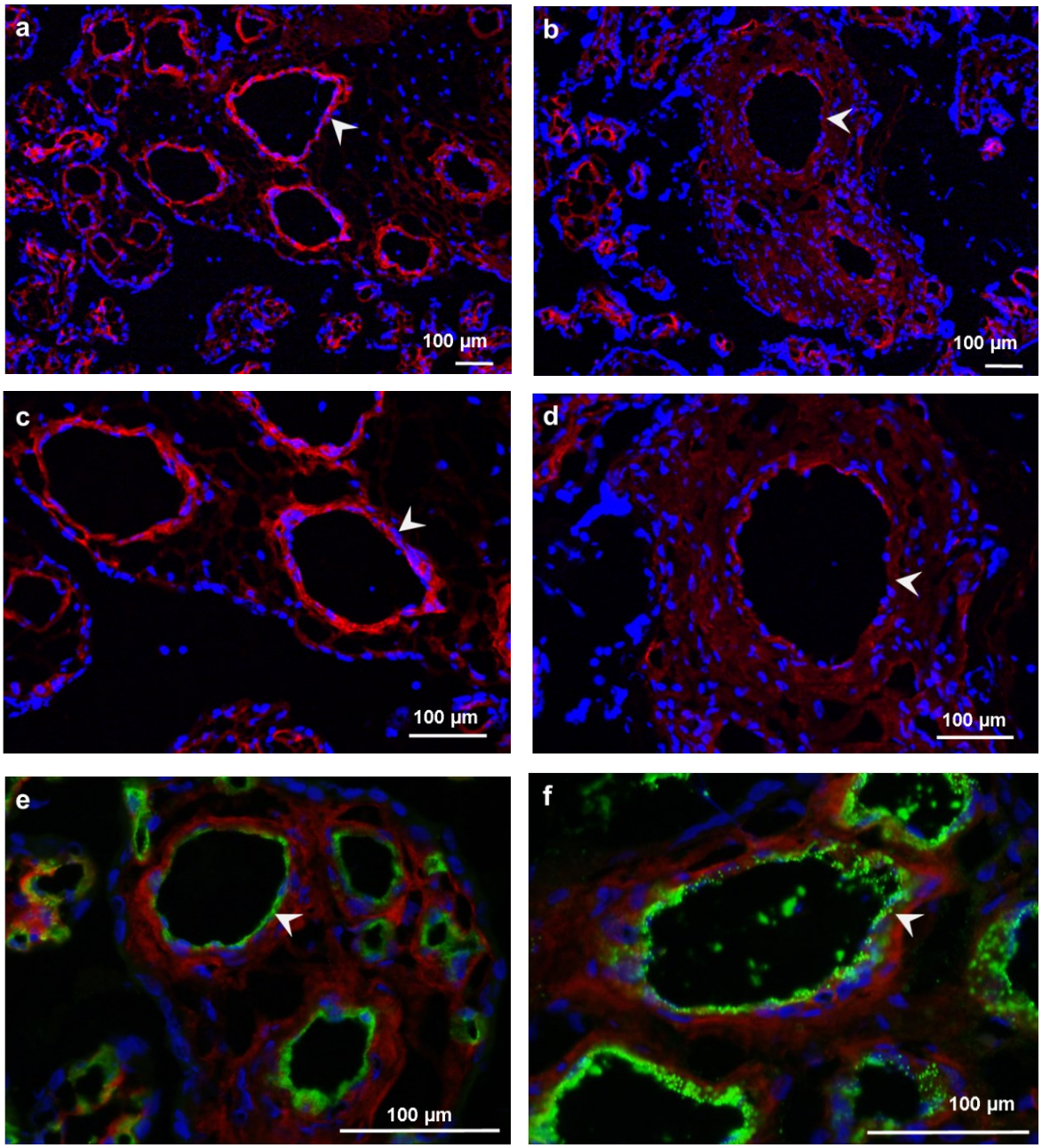

Figure 10. Immunolocalization of versican in human term placenta.

Cryosections of placental tissue of control (**a**, **c**, **e** and **f**) and GDM (**b** and **d**) pregnancies were stained with versican (V0) antibody (showed in red), DAPI for nuclei and CD34 (**e**) or von Willebrand factor antibody (**f**) for endothelial cells (green). Subendothelial layers are marked with white arrowheads (**a**, **b**, **c**, **d**).

In addition, protein levels of versican V0 in cord blood serum after healthy pregnancies (control CBS) and pregnancies complicated with gestational diabetes (GDM CBS) were evaluated by ELISA, revealing lower levels of versican V0 in GDM CBS compared to control CBS (**Figure 11**).

Since immunostaining exhibited the presence of versican V0 in stromal cells, evaluation of the expression of versican and its binding partners in different cell types and fetal tissues isolated and available in our laboratory was of interest.

VCAN V0 expression was higher in placental venous endothelial cells (VEC) $p<0.001$, in human umbilical vein endothelial cells (HUVEC) ($p<0.01$), and in placental smooth muscle cells (SMC) ($p<0.001$) when compared to control AEC (**Figure 12a**). *VCAN V1* expression was higher in SMC ($p<0.001$) than in AEC (**Figure 12b**). Expression of *VCAN V2* was higher in HUVEC ($p<0.05$) and SMC ($p<0.001$) than in AEC (**Figure 12c**), whereas *VCAN V3* expression was only higher in SMC ($p<0.001$) (**Figure 12d**).

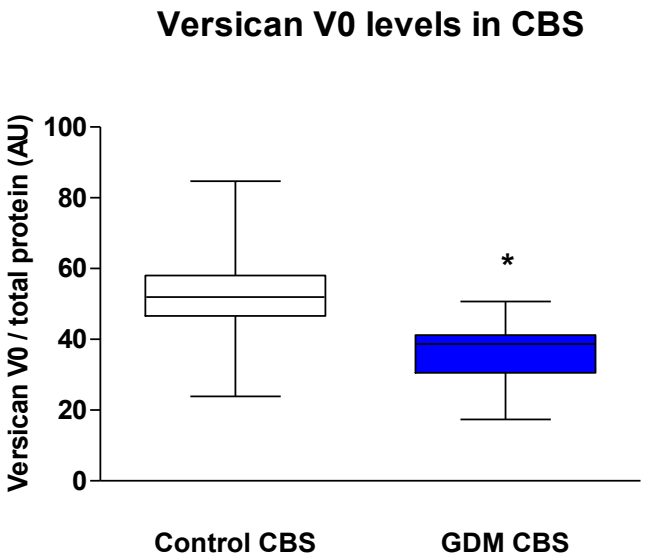

Figure 11. **Protein levels of versican V0 in cord blood serum determined by ELISA.** Levels of total versican determined by ELISA in cord blood serum (CBS) after healthy (control CBS) and pregnancies complicated with gestational diabetes (GDM CBS). Values were normalized to total protein content ($n_{control\ CBS} = 8$; $n_{GDM\ CBS} = 7$). *$p<0.05$

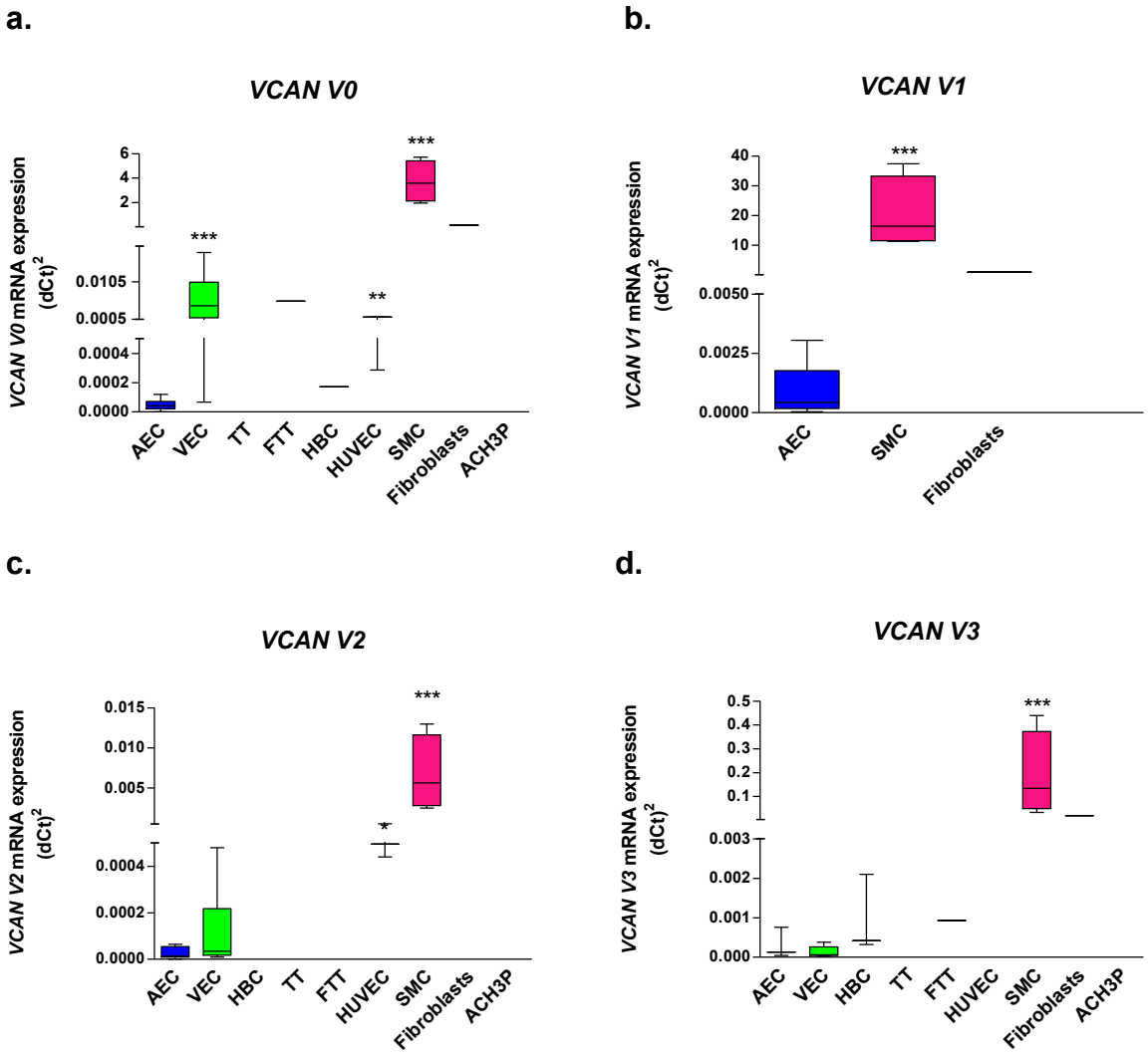

Figure 12. mRNA expression of versican isoforms in human placental cells.

mRNA expression of versican in AEC, venous placental endothelial cells (VEC), placental macrophages (HBC), term trophoblasts (TT), first trimester trophoblasts (FTT), human umbilical vein endothelial cells (HUVEC), smooth muscle cells (SMC), fibroblasts and ACH3P. ($n_{AEC} = 16$; $n_{VEC} = 14$; $n_{HBC} = 3$; $n_{TT} = 4$; $n_{FTT} = 7$; $n_{HUVEC} = 5$; $n_{SMC} = 4$; $n_{Fibroblasts} = 1$; $n_{ACH3P} = 2$). *p<0.05; **p<0.01; ***p<0.001

FBN1 expression was higher in VEC ($p<0.001$), term trophoblasts ($p<0.001$), and first trimester trophoblasts ($p<0.001$), compared to AEC. While, in HBC ($p<0.001$) and ACH3P ($p<0.001$) was decreased compared to AEC (**Figure 13a**). *TGFβI* expression was higher in VEC ($p<0.001$), than in AEC. Whereas, in term trophoblasts ($p<0.01$), first trimester trophoblasts ($p<0.05$), HUVEC ($p<0.01$) and ACH3P ($p<0.001$), *TGFβI* expression was lower than in AEC (**Figure 13b**). *TGFβ1* expression was higer in first trimester trophoblast ($p<0.05$), compared to AEC. Whereas, it was lower in HBC ($p<0.001$), term trophoblasts ($p<0.001$) and ACH3P, than in AEC (**Figure 13c**).

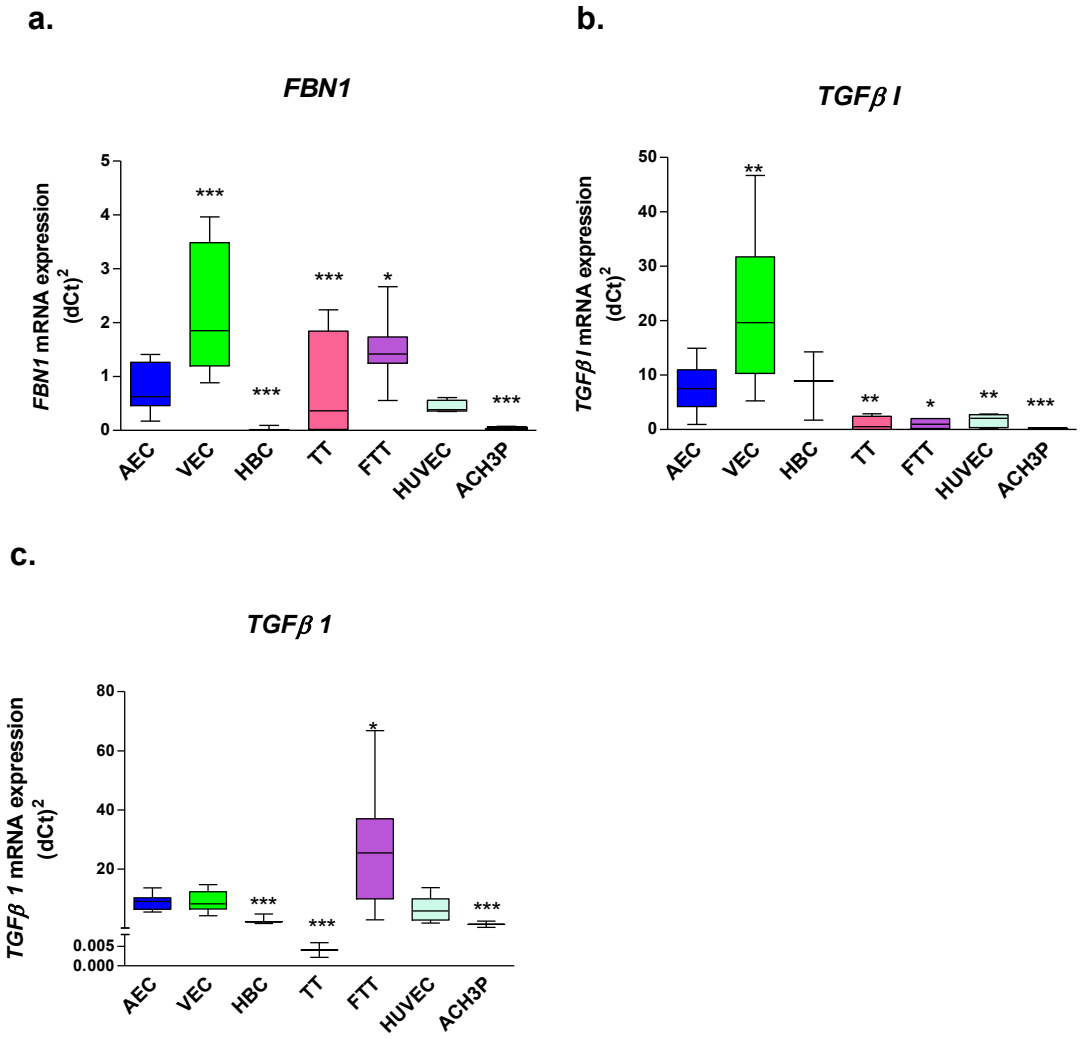

Figure 13. mRNA expression of *FBN1*, *TGFβI* & *TGFβ1* in human placental cells.

mRNA expression of *FBN1*, *TGFβI* & *TGFβ1* in AEC, VEC, HBC, term trophoblasts (TT), first trimester trophoblasts (FTT), HUVEC, SMC, fibroblasts and ACH3P. (n_{AEC} = 16; n_{VEC} = 14; n_{HBC} = 3; n_{TT} = 4; n_{FTT}= 7; n_{HUVEC} = 5; n_{SMC} = 4; $n_{Fibroblasts}$ = 1; n_{ACH3P} = 2). *p<0.05; **p<0.01; ***p<0.001

Expression of *VCAN V0* was higher in first trimester placenta compared to term placenta ($p<0.01$), whereas expression in other fetal organs was lower, although in kidney no difference was observed (**Figure 14a**). Only one placental sample expressed *VCAN V2*, and first trimester placenta showed similar expression levels. Fetal kidney, thymus and heart revealed decreased levels compared to placenta, while fetal brain exhibited higher levels than placenta (**Figure 14b**). *VCAN V3* expression showed no differences (**Figure 14c**).

FBN1 expression was higher in term placenta than in all other tissues evaluated (**Figure 15a**). *TGFβI* expression was similar in placental tissues, while decreased levels were found in other fetal tissues (**Figure 15b**). *TGFβI* expression was higher in term compared to first trimester placental tissue ($p<0.001$), and to all other fetal tissues evaluated (**Figure 15c**).

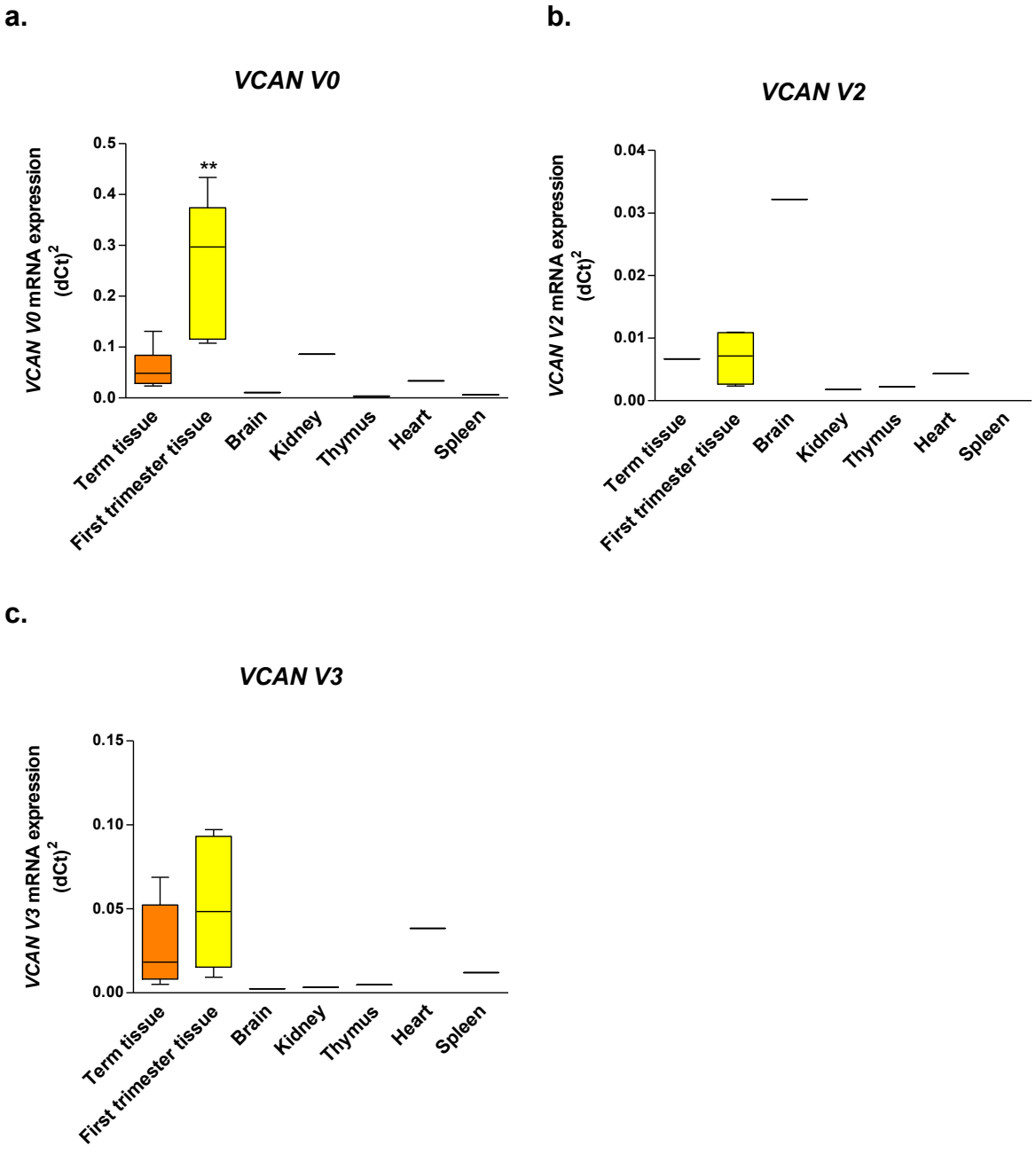

Figure 14. mRNA expression of versican isoforms in human fetal tissues.

mRNA expression of versican in human term placental tissue (n=6), first trimester placental tissue (n=6), and brain, kidney, thymus, heart and spleen of fetal origin (Clontech human fetal RNA pools). **p<0.01

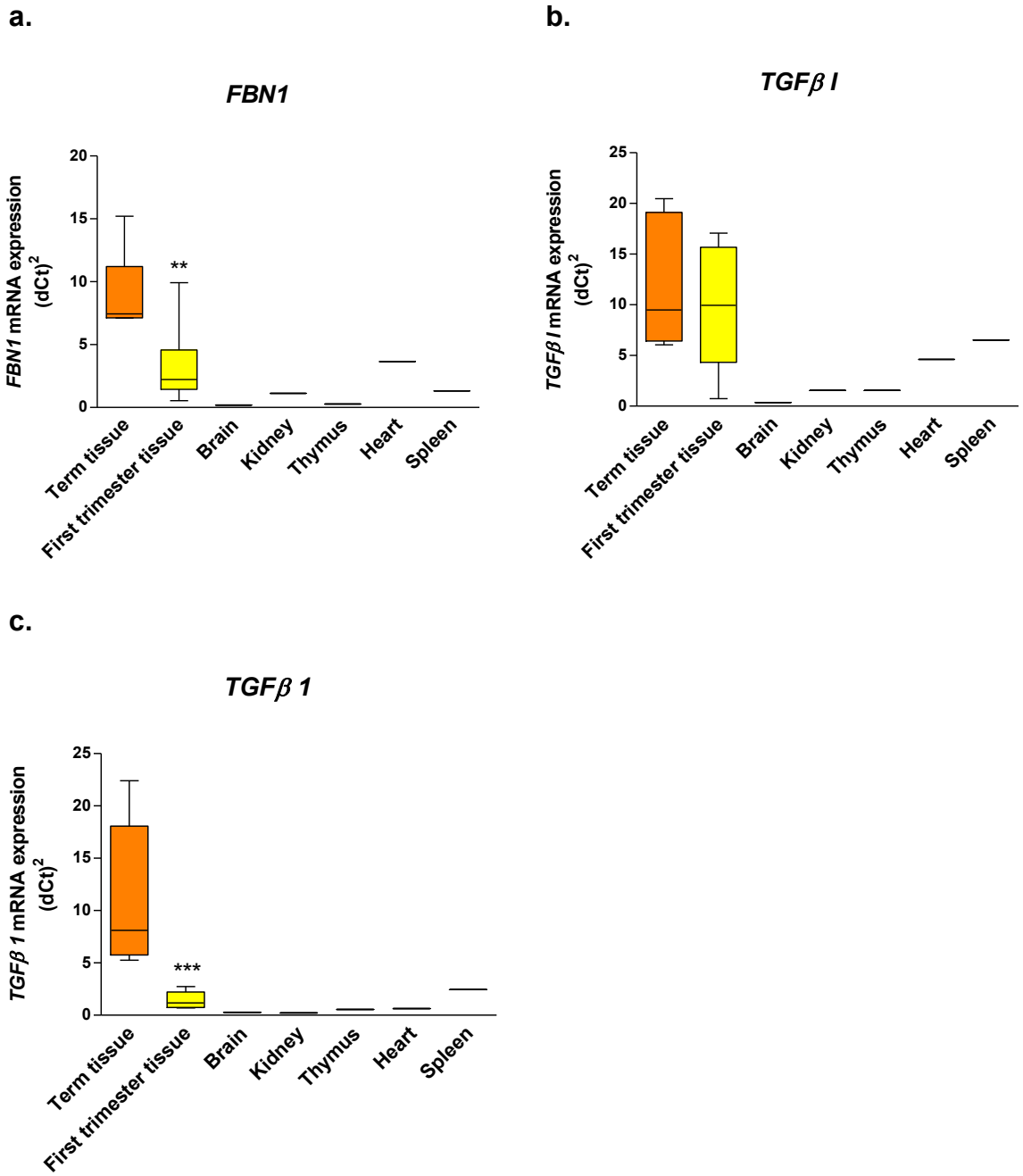

Figure 15. mRNA expression of *FBN1*, *TGFβI* & *TGFβ1* in human fetal tissues.

Expression of *FBN1*, *TGFβI* & *TGFβ1* in human term placental tissue (n=6), first trimester placental tissue (n=6), and brain, kidney, thymus, heart and spleen of fetal origin (Clontech human fetal RNA pools). **p<0.01; ***p<0.001

Moreover, GDM effect in placental cells and tissue was evaluated, revealing increased *VCAN V0* expression in AEC ($p<0.001$) after GDM (**Figure 16a**). *VCAN V1* expression was increased in GDM AEC compared to control AEC ($p<0.001$) (**Figure 16b**) *VCAN V2* expression was increased in AEC $p<0.001$ and decreased in SMC ($p<0.001$) after GDM (**Figure 16c**). *VCAN V3* expression was increased in VEC after GDM ($p<0.001$) (**Figure 16d**).

Increased *FBN1* expression in AEC ($p<0.001$), and term trophoblasts ($p<0.05$) after GDM (**Figure 17a**) was found. Expression of *TGFβI* was higher in AEC ($p<0.01$) and decreased in VEC after GDM ($p<0.01$) (**Figure 17b**). GDM decreased *TGFβ1* expression in VEC ($p<0.001$), and term placental tissue ($p<0.01$) (**Figure 17c**).

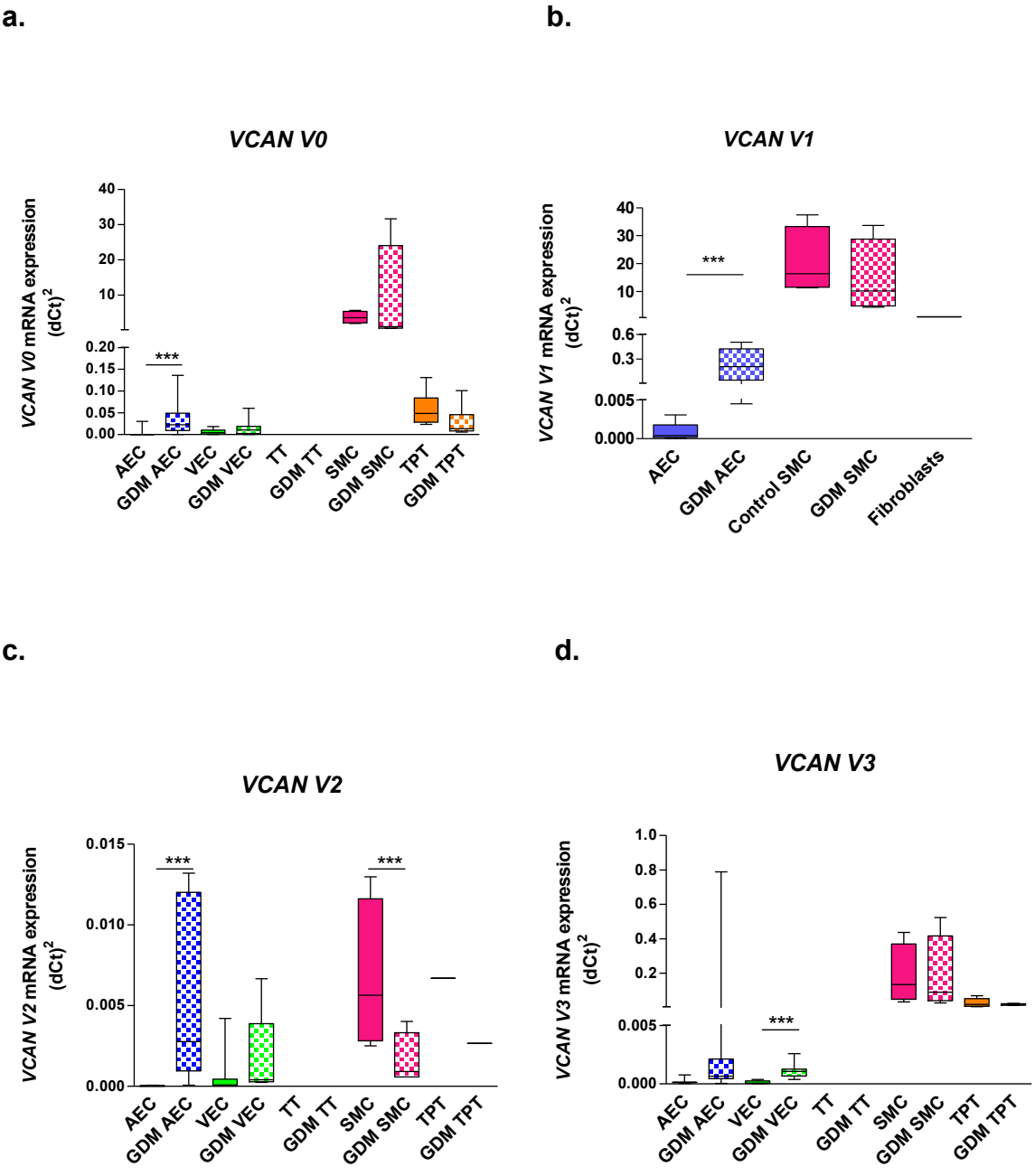

Figure 16. Effect of GDM on versican expression in human placental cells and tissue. mRNA expression of versican in control and GDM AEC, control and GDM VEC, control term trophoblast (TT), GDM trophoblast (GDM TT), control and GDM SMC, control term placental tissue (TPT) and GDM term placental tissue (GDM TPT). (n_{AEC} = 12; $n_{GDM\ AEC}$ = 14; n_{VEC} = 12; $n_{GDM\ VEC}$ = 8; n_{TT} = 4; $n_{GDM\ TT}$ = 4; n_{SMC} = 4; $n_{GDM\ SMC}$ = 4; n_{TPT} = 6; $n_{GDM\ TPT}$ = 6). ***p<0.001

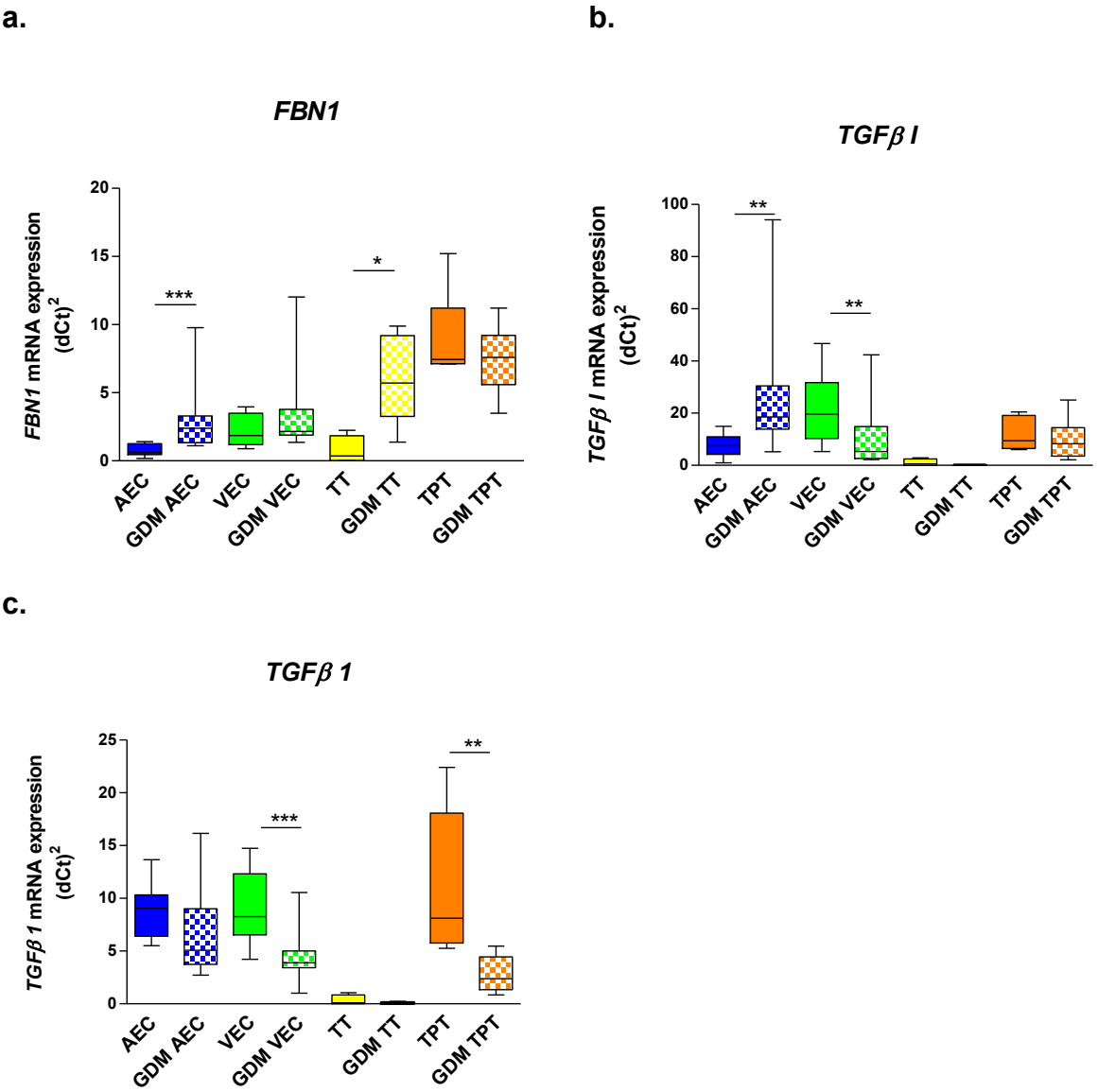

Figure 17. Effect of GDM on *FBN1*, *TGFβI* & *TGFβ1* expression in placental cells and tissue.

Expression of *FBN1*, *TGFβI* & *TGFβ1* in control and GDM AEC, control and GDM VEC, control term trophoblast (TT), GDM trophoblast (GDM TT), control and GDM SMC, control term placental tissue (TPT) and GDM term placental tissue (GDM TPT) was evaluated by RT-qPCR (n_{AEC} = 12; $n_{GDM\ AEC}$ = 14; n_{VEC} = 12; $n_{GDM\ VEC}$ = 8; n_{TT} = 4; $n_{GDM\ TT}$ = 4; n_{SMC} = 4; $n_{GDM\ SMC}$ = 4; n_{TPT} = 6; $n_{GDM\ TPT}$ = 6). *p<0.05; **p<0.01; ***p<0.001

2. Identify whether the pro-inflammatory components of the fetal GDM environment alter endothelial function.

Nitric oxide evaluation: transcript and bioavailability

Since NO plays an essential role in endothelial function, expression of endothelial nitric oxide synthase (eNOS) was evaluated on the transcript level (**Figure 18a**), resulting in 2-fold change upregulation in GDM compared to control AEC ($p<0.052$). As this tendency was close to significance, NO bioavailability was measured. After stimulating both control and GDM AEC with insulin, NO availability increased by 33% in control AEC ($p<0.001$) and by 32% in GDM AEC ($p<0.001$). Treatment with L-NAME (a specific inhibitor for the nitric oxide synthase) decreased intracellular nitric oxide bioavailability by 46% in control AEC ($p<0.001$), and by 51% in GDM AEC. Treatment of cells with L-NAME before stimulation with insulin did not show any significant change compared to the basal bioavailability of NO (**Figure 18b**). There was no difference in NO bioavailability or eNOS transcription between control and GDM AEC in any of the treatments.

a.

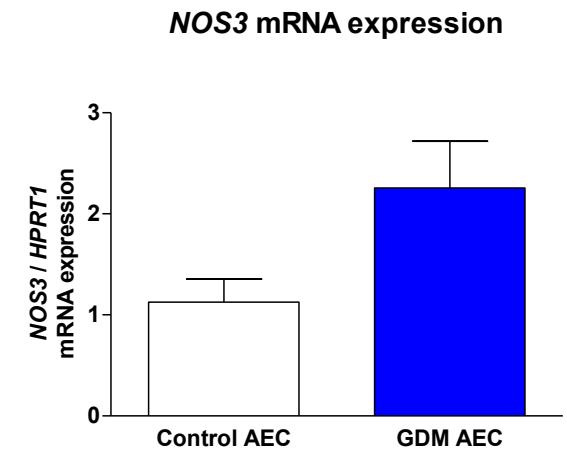

b.

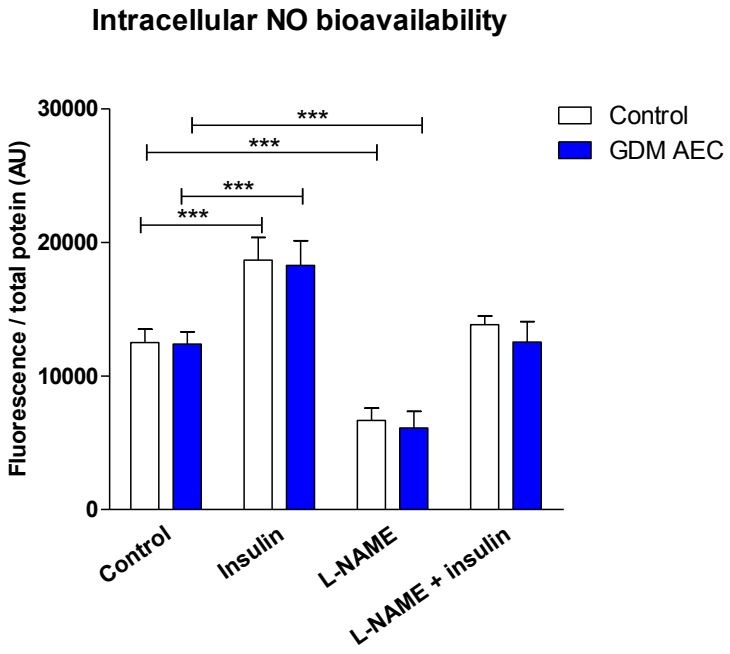

Figure 18. Nitric oxide evaluation.

a. *NOS3* mRNA expression, RT-qPCR was determined by RT-qPCR ($n_{control\ AEC} = 7$; $n_{GDM\ AEC} = 7$; p=0.052). NO bioavailability in control and GDM AEC was evaluated using a fluorescent probe DAF-FM diacetate and fluorescence was measured and represented in (**b**) ($n_{control\ AEC} = 5$, $n_{GDM\ AEC} = 5$; technical triplicates). ***p<0.001. Modified from 'Hyperinsulinemia stimulates angiogenesis of human fetoplacental endothelial cells: a possible role of insulin in placental hypervascularization in diabetes mellitus' (Lassance et al., 2013).

Cell adhesion molecules

Expression of classical markers for endothelial dysfunction in AEC after healthy and GDM pregnancies was evaluated. Evaluation of mRNA by RT-qPCR showed no difference in expression of *ICAM-1* (**Figure 19a**), *E-selectin* (**Figure 19b**) or *VCAM-1* (**Figure 19c**). Whereas, immunoblotting for cellular ICAM-1 protein revealed a decreasing trend of ICAM-1 levels in GDM AEC (**Figure 19d**) (-28.5%; p=0.07). No differences were found in levels of E-selectin (**Figure 19e**) or VCAM-1 (**Figure 19f**). FACS analysis revealed decreased levels of membrane bound ICAM-1 in GDM AEC (**Figure 19g**) (-73%; p<0.001). Membrane E-selectin and VCAM-1 were not detected by FACS (data not shown).

Since ICAM-1 was decreased in GDM derived AEC, further analyses of ICAM-1 protein were performed. Secreted soluble ICAM-1 (sICAM-1) levels were determined by ELISA in supernatant of cultured AEC. No significant difference was detected between control and GDM AEC (**Figure 20a**). However, there was a tendency for lower sICAM-1 secretion in AEC after GDM pregnancy (-56%; p=0.07). Unaltered levels of sICAM-1 were found in cord blood serum (CBS) after control and GDM pregnancies (**Figure 20b**).

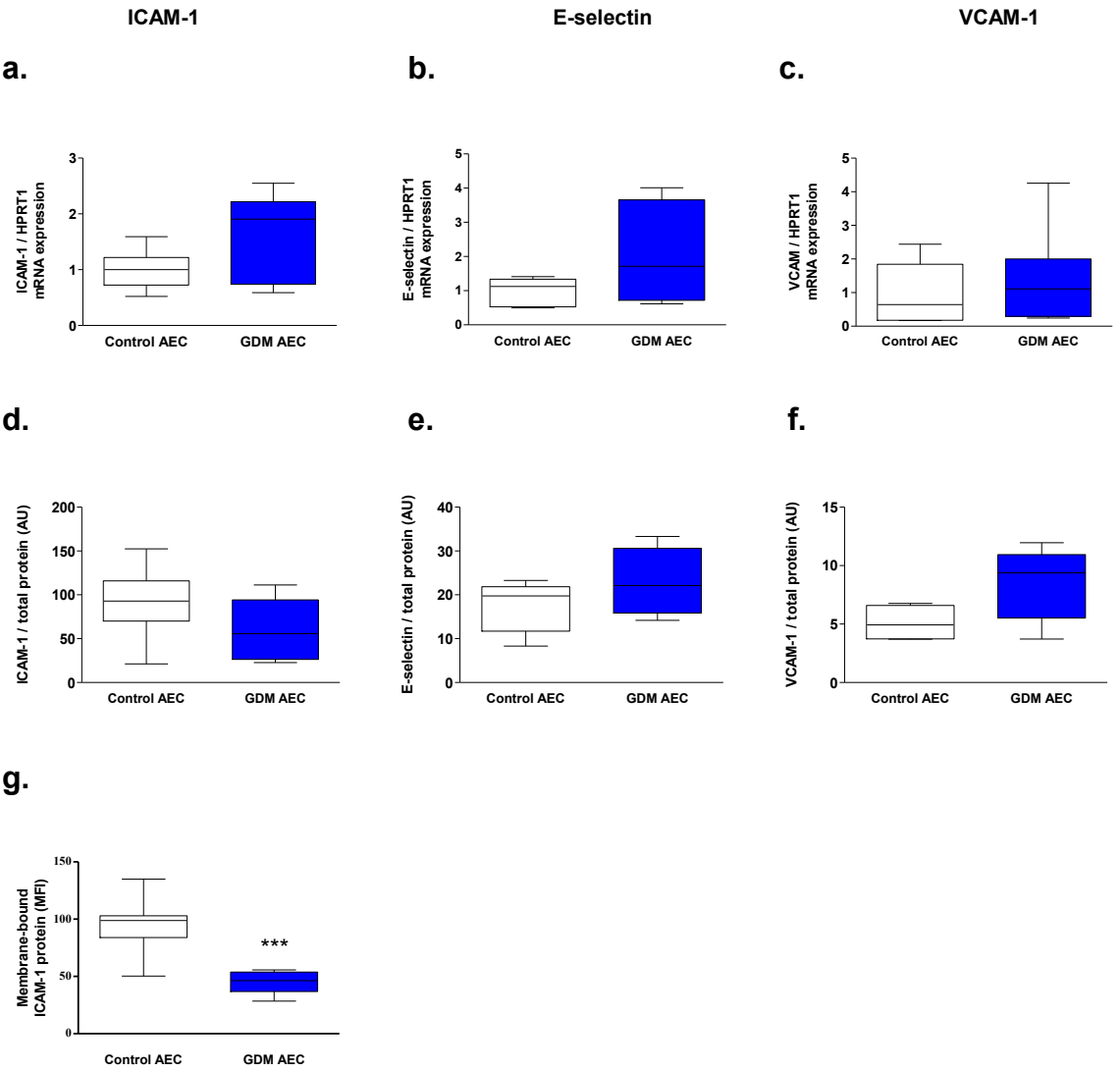

Figure 19. Cell adhesion molecules mRNA and protein expression in human placental arterial endothelial cells.

mRNA expression of *ICAM-1* (**a**), *E-selectin* (**b**) or *VCAM-1* (**c**) in control vs. GDM AEC ($n_{control\ AEC}$ = 7, $n_{GDM\ AEC}$ = 7). Immunoblot for ICAM-1 (**d**) ($n_{control\ AEC}$ = 19, $n_{GDM\ AEC}$ = 11; p=0.07), E-selectin ($n_{control\ AEC}$ = 5, $n_{GDM\ AEC}$ = 5) (**e**) and VCAM-1 ($n_{control\ AEC}$ = 5, $n_{GDM\ AEC}$ = 5) (**f**) in control vs. GDM AEC. FACS analysis of membrane-bound ICAM-1 ($n_{control\ AEC}$ = 8, $n_{GDM\ AEC}$ = 8) (**g**). Membrane bound E-selectin and membrane bound VCAM-1 were not detected by FACS (data not shown). ***p<0.001. Modified from 'Post-transcriptional down regulation of ICAM-1 in feto-placental endothelium in GDM' (Díaz-Pérez et al., 2016).

a.

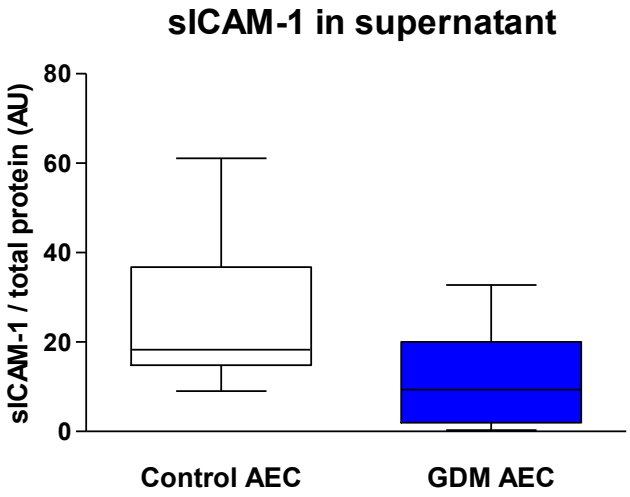

b.

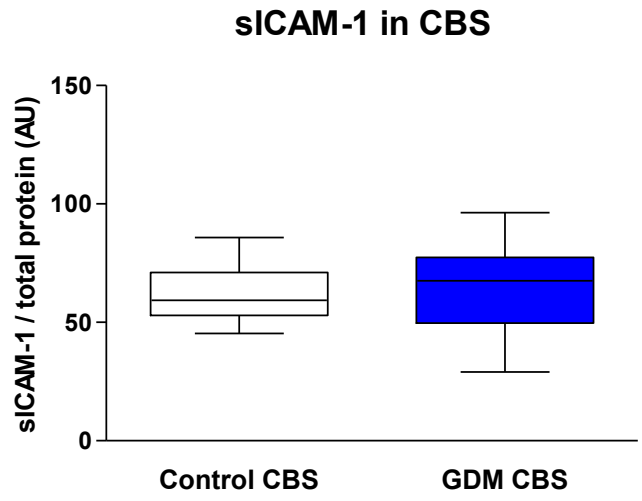

Figure 20. sICAM-1 levels in supernatant of cultured human placental arterial endothelial cells and cord blood serum after healthy and GDM pregnancies.

Secreted ICAM-1 measured by ELISA in supernatant of cultured control and GDM AEC ($n_{control\ AEC} = 12$; $n_{GDM\ AEC} = 6$; p=0.07) (**a**). Levels of sICAM-1 in cord blood serum (CBS) after control and GDM pregnancies ($n_{control\ CBS} = 12$; $n_{GDM\ CBS} = 17$) (**b**). Modified from 'Post-transcriptional down regulation of ICAM-1 in feto-placental endothelium in GDM' (Díaz-Pérez et al., 2016).

Examination of human term placenta located ICAM-1 in feto-placental endothelium and in Hofbauer cells (HBC) was performed by immunohistochemistry. Less intense ICAM-1 staining was found in placental tissue after GDM pregnancies compared to placental tissue of control pregnancies (**Figure 21**).

Since ICAM-1 interacts with membrane-bound β2 integrin receptors CD11a/CD18 (LFA-1) and CD11b/CD18 (Mac-1), placental tissue sections were stained for CD11a and CD18 to distinguish possible ICAM-1 mediated binding partners for the feto-placental endothelium. Immunohistochemistry revealed fetal blood cells as main ICAM-1 binding partners since they showed positive staining for CD11 (**Figures 22a** & **Figure 22b**) and for CD18 (**Figures 22c** & **Figure 22d**). Placental Hofbauer cells also expressed CD11 (**Figure 22c**).

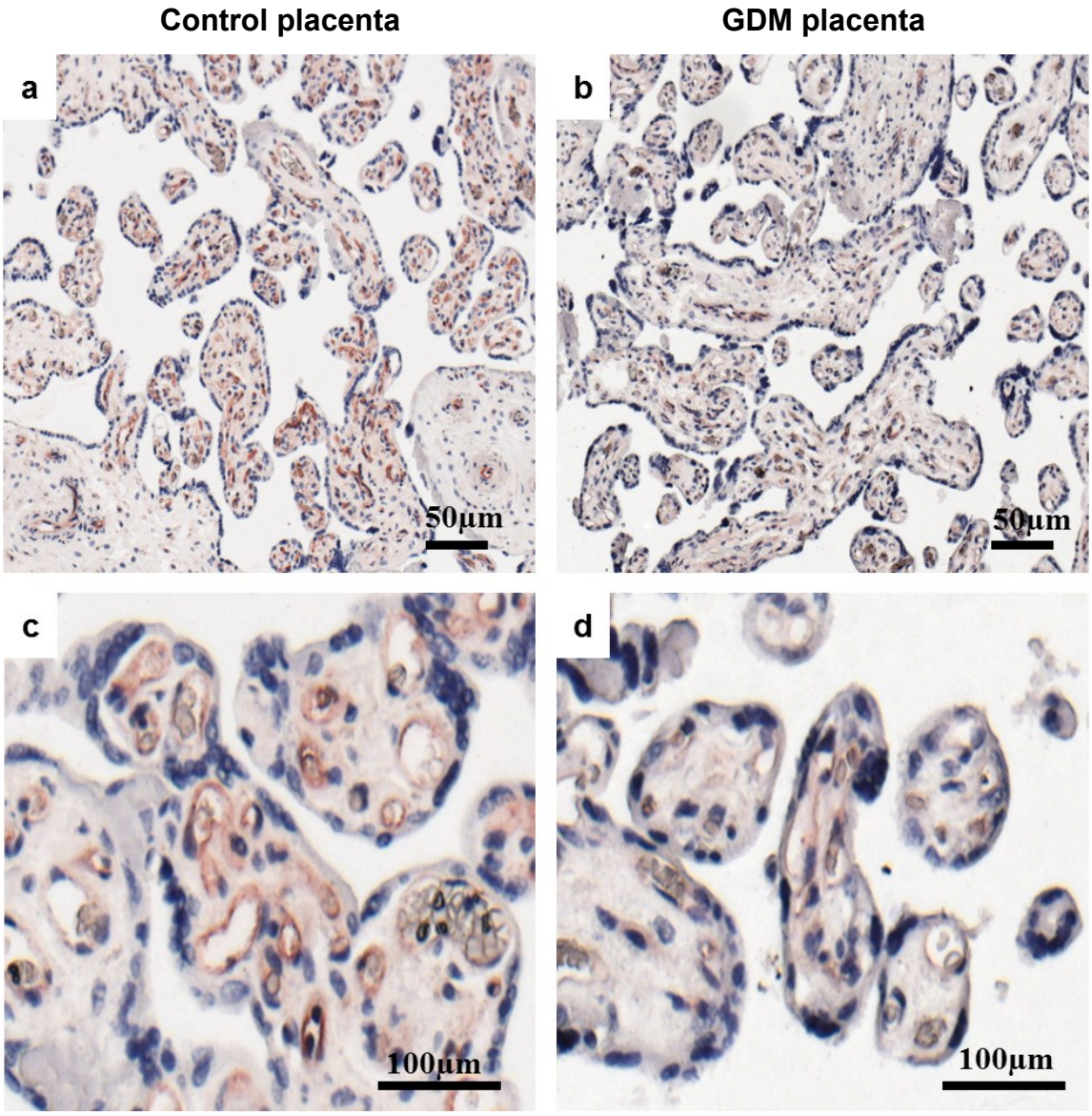

Figure 21. Immunolocalization of ICAM-1 in human term placenta after healthy and GDM pregnancies.

Placental tissue after healthy (**a**, **c**) and GDM pregnancies (**b**, **d**) were imunostained for ICAM-1 (shown in red). Nuclei were stained with DAPI (blue). Representative pictures of Control (n = 4) and GDM (n = 3) human term placentas. Modified from 'Post-transcriptional down regulation of ICAM-1 in feto-placental endothelium in GDM' (Díaz-Pérez et al., 2016).

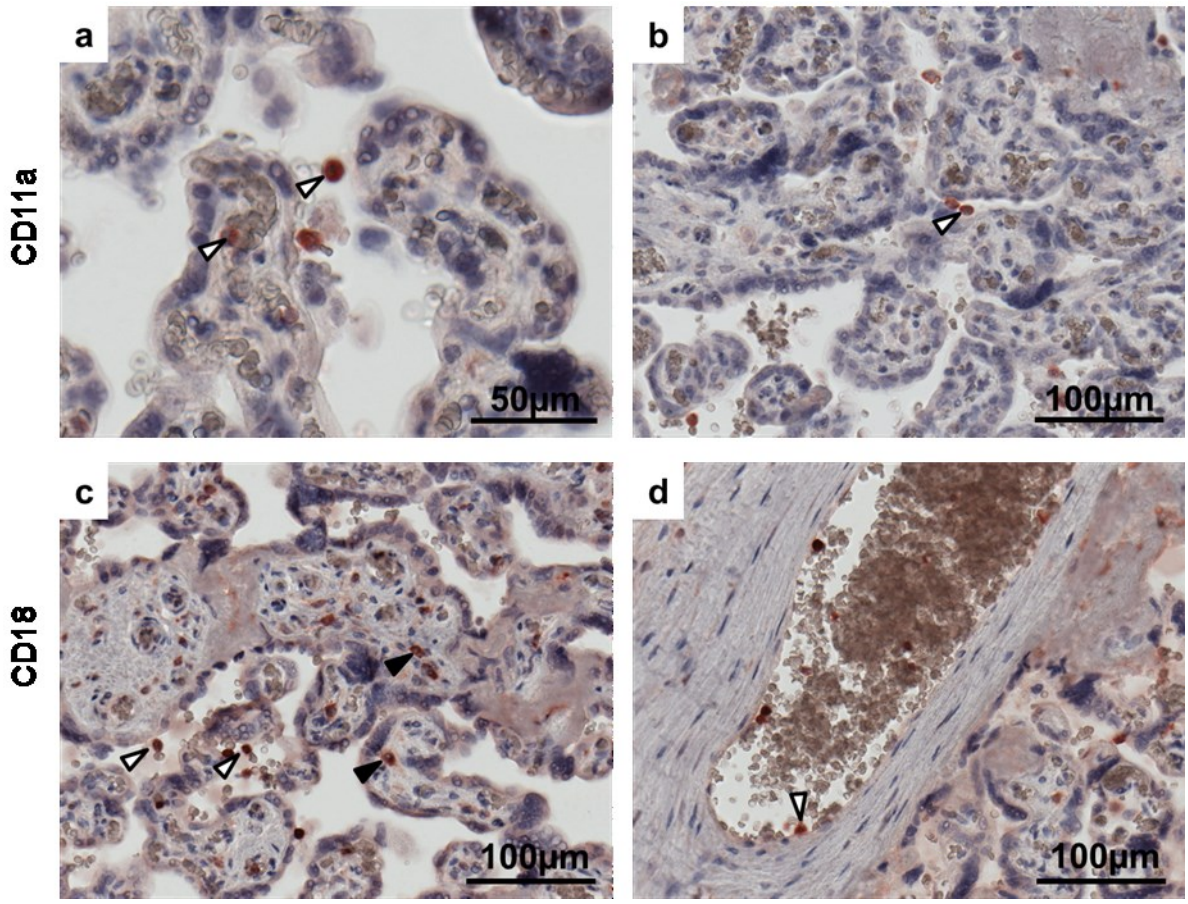

Figure 22. Immunolocalization of ICAM-1 binding partners CD11a and CD18 subunits of LFA-1 in human term placenta after healthy pregnancy.

Expression Placental tissue after healthy pregnancies stained for CD11a (**a**, **b**) and CD18 (**c**, **d**) in red. Nuclei were stained with DAPI (blue). White arrowheads indicate maternal and fetal blood cells are indicated with, and black arrowheads indicate Hofbauer cells. Representative pictures of 4 control placentas are shown. Modified from 'Post-transcriptional down regulation of ICAM-1 in feto-placental endothelium in GDM' (Díaz-Pérez et al., 2016).

Angiogenesis

Since angiogenesis is an essential property of the endothelium, angiogenic capacity of the AEC was studied. Endothelial proliferation and migration are key steps in angiogenesis. Thus, cell cycle proteins expression was evaluated.

Cell cycle regulators

Data previously generated by protein array revealed increased protein levels of CDC47 (1.7-fold), Cyclin-dependent kinase 5 (1.9-fold), Cullin1 (1.8-fold), Cullin3 (1.5-fold), p27 (1.5-fold) and 14.3.3 η (1.9-fold; p=0.05) in GDM AEC compared to control AEC. Due to the gender differences found, only female samples were used in all further experiments. Under these culture conditions only *DNMT1* exhibited an increased expression in GDM AEC compared to control AEC (**Table 6**). However, no significant differences were found by immunoblot (**Figure 23**).

Table 6. RT-qPCR for selecting target proteins.

Cells cultured with 5% FCS EBM media without supplements for 48 hours at 21% O_2 & 37°C, gene expression was normalized to *HPRT1*.

Gene	Fold change Control vs. GDM AECs	p-value
DNMT1	1.19	0.037
VCAN	1.41	0.060
RAD51	1.47	0.077
IL6	1.47	0.095
GJA5	1.72	0.121
GADD45A	1.63	0.133
CDK2	1.15	0.159
GADD45B	1.35	0.180
CHEK1	1.31	0.265
ANGPT2	0.54	0.280
CUL3	1.11	0.305
NOTCH4	1.14	0.318
CDC14A	0.65	0.325
CDK4	1.05	0.338
CCNC	1.54	0.387
CDKN1B	0.81	0.399
GSK3B	1.05	0.427
CTNNB1	1.09	0.496
IL8	0.91	0.537
YWHAH	0.92	0.566
CDK1	1.13	0.575
CDK5	1.11	0.682
CDK8	1.15	0.814

ABR	1.13	0.855
CCND2	0.93	0.856
CDKN1C	0.90	0.856
CUL1	1.00	0.860
CDKN1A	0.97	0.892
CDC47	1.16	0.898
H19	0.91	0.974

a.

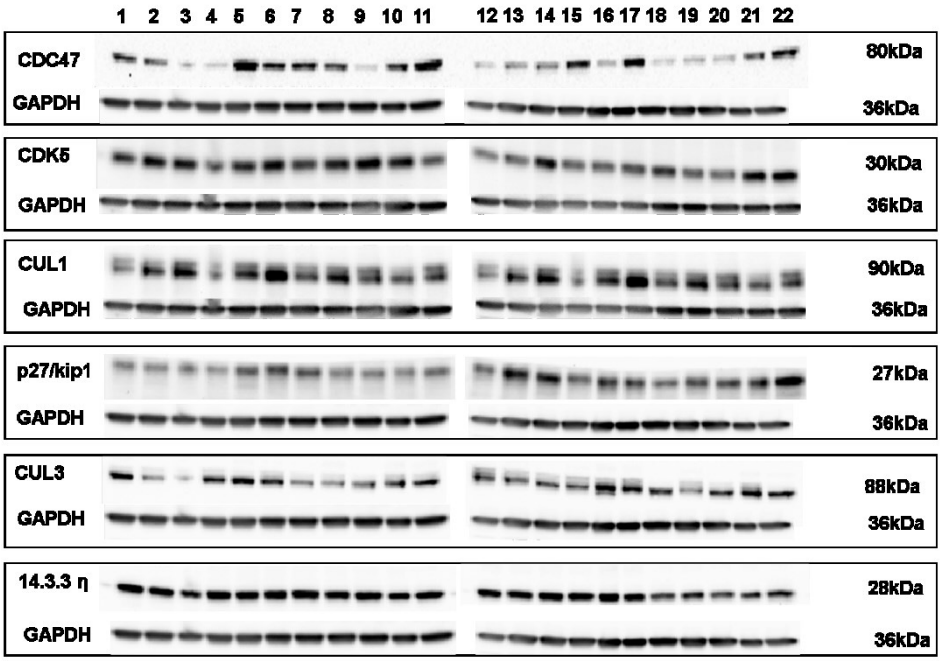

b.

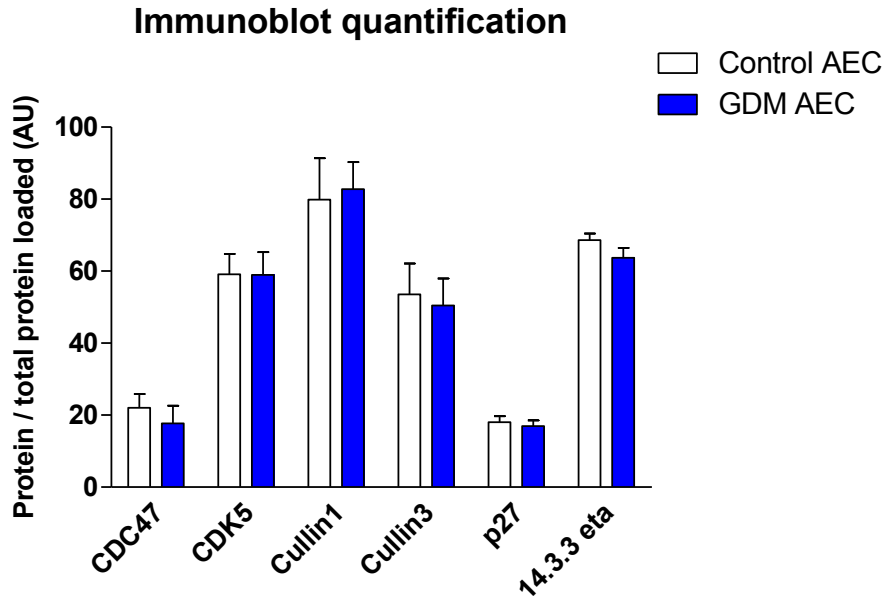

Figure 23. Protein expression of cell cycle regulators in control and GDM AECs.

a. Immunoblot for cell cycle proteins; lanes 1, 3, 5, 7, 9, 11, 12, 14, 16, 18, 20 are GDM AEC samples, while lanes 2, 4, 6, 8, 10, 13, 15, 17, 19, 21 and 22 are control AEC. Lanes 10 and 21 is the internal control for comparing membrane 1 and membrane 2. Quantification of the signal intensities are represented in **b** ($n_{control\ AEC}$ =10; $n_{GDM\ AEC}$ = 11).

Furthermore, cell cycle proteins CDK4 and Cyclin-D2 were found to concordantly differ on mRNA and gene methylation levels in AEC after GDM pregnancies. Thus, protein levels were evaluated by immunoblot and ELISA. Protein levels of Cyclin-D2 measured by ELISA were found to be 1.8-fold higher ($p<0.01$) in GDM AEC compared to control AEC (**Figure 24a**). ELISA for total CDK4 (**Figure 24b**) revealed a decrease in CDK4 levels in GDM AEC by 42% compared to control AEC ($p<0.01$).

a.

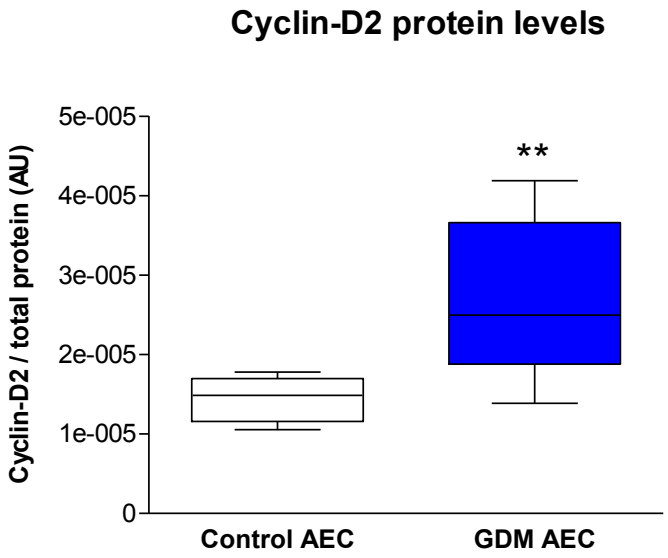

b.

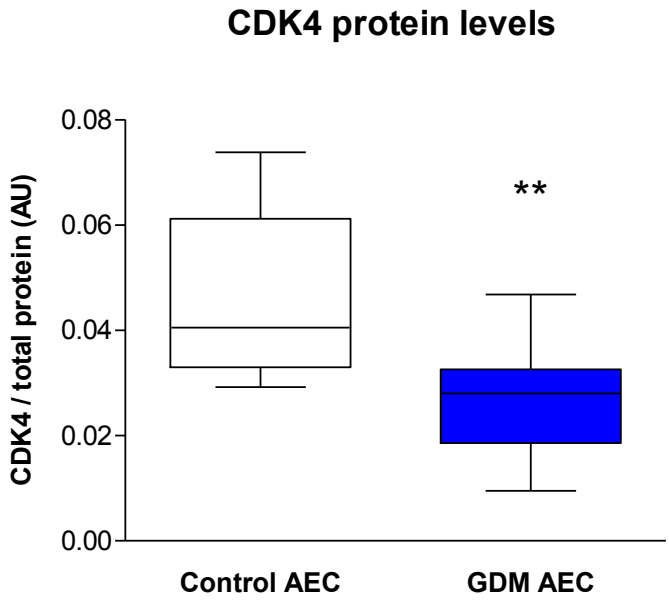

Figure 24. Cyclin-D2 & CDK4 protein expression.

a. Protein levels of cyclin-D2 were determined by ELISA ($n_{control\ AEC}$= 8; $n_{GDM\ AEC}$ = 8). **b.** CDK4 protein levels measured by ELISA ($n_{control\ AEC}$ = 9; $n_{GDM\ AEC}$ = 9). Protein levels were normalized to the total protein content. **p<0.01

The angiogenic potential of AEC was evaluated by quantifying the formation of tubes onto fibrin matrices. *In vitro* tube formation of control and GDM AEC was higher after stimulation with VEGF, TNFα and combinations of VEGF/TNFα, VEGF/TGFβ1 and VEGF/TNFα/TGFβ1 compared to untreated AEC. Tube formation of GDM AEC was lower than control AEC after stimulation with VEGF, TNFα, VEGF/TNFα, VEGF/TGFβ1 and VEGF/TNFα/TGFβ1 (**Figure 25**), being VEGF/TNFα the most effective *stimuli* for tube formation on both, control and GDM AEC.

Since versican was of interest, its mRNA expression and protein levels were determined after exposing control AEC to combinations of VEGF (10ng/ml), TGFβ1 (50pg/ml) and or TNFα (10µg/ml), revealing decreased *VCAN* mRNA after treatment of VEGF alone and in combination with TGFβ1 and or TNFα (**Figure 26a**), while protein levels of versican in supernatant decreased in all AEC isolations evaluated only after VEGF/TNFα treatment (**Figure 26b**). Thus, further experiments were performed using VEGF/TNFα (VT) treatment as a positive control for tube-formation.

Protein levels of fibrillin1 and TGFβI were also determined after exposing control AEC to combinations of VEGF (10ng/ml), TGFβ1 (50pg/ml) and or TNFα (10µg/ml). Interestingly, levels of fibrillin1 decreased only in presence of VEGF (**Figure 27a**), while evaluation of TGFβ1 did not show a pattern due to intra-population variability (**Figure 27a**).

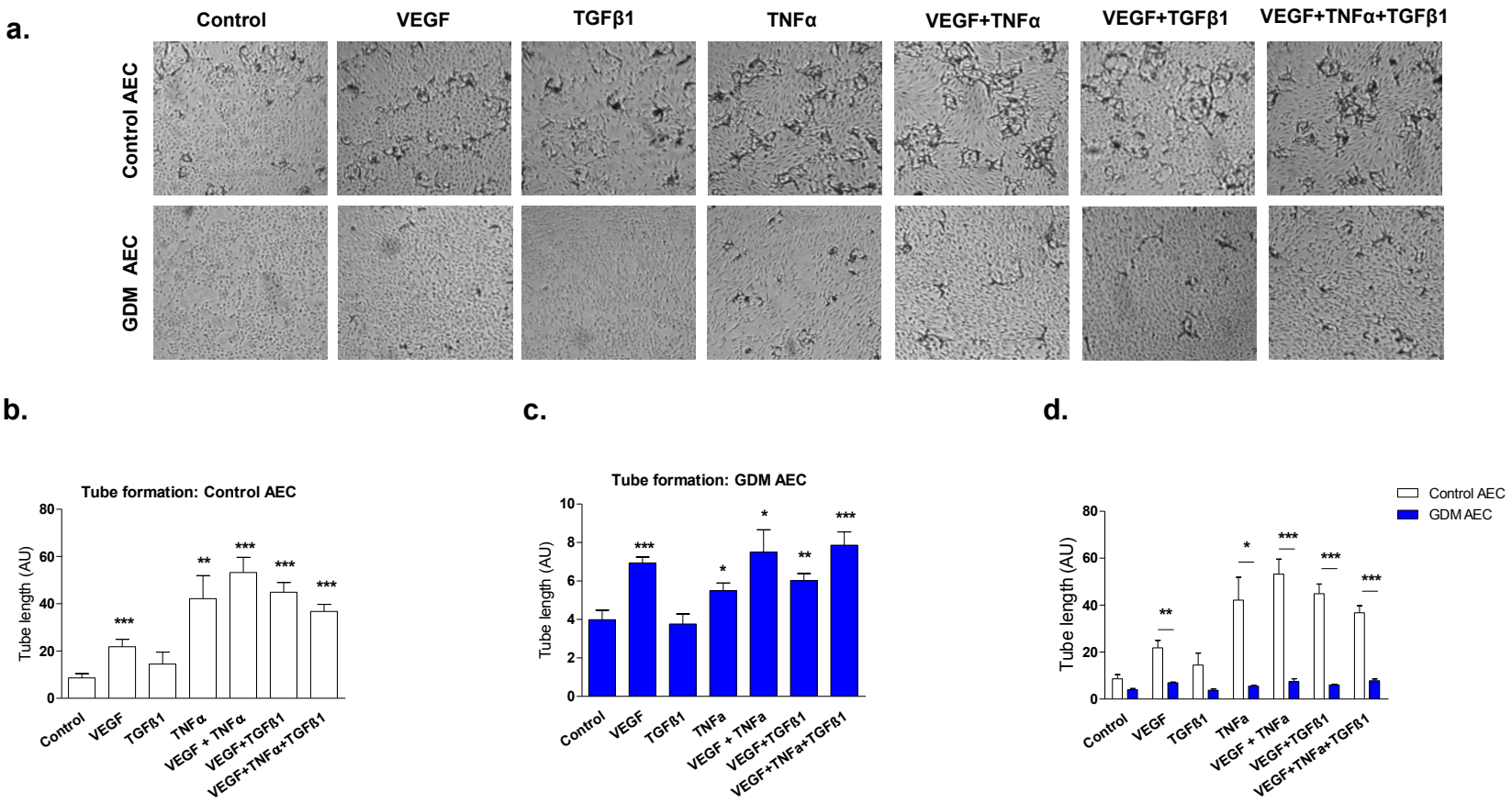

Figure 25. *In vitro* tube formation of human placental arterial endothelial cells.

(**a**) *In vitro* tube formation of control and GDM AEC in absence or presence of VEGF (10ng/ml), TGFβ1 (50pg/ml) and TNFα (10µg/ml). Quantification of control AEC (**b**) and GDM AEC (**c**) separated and together (**d**). Quantification of pictures on 2.5X magnification was performed with Optimas 6.5. Representative pictures of quadruplicates are shown ($n_{control\ AEC}$=4; $n_{GDM\ AEC}$=2) Note: 3/5 GDM AEC isolations did not respond to any stimulation, and thus were not used in the present analysis. * p<0.05; **p<0.01; ***p<0.001

a.

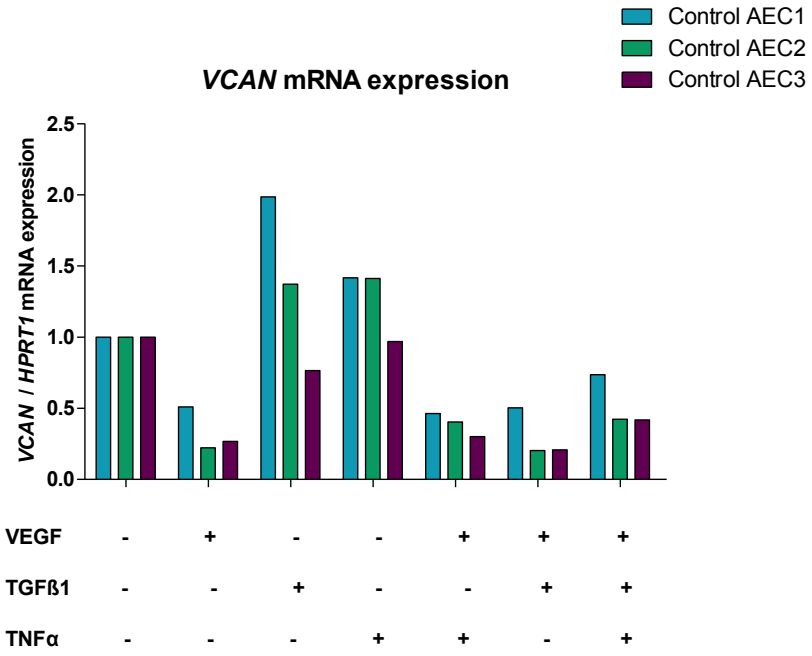

b.

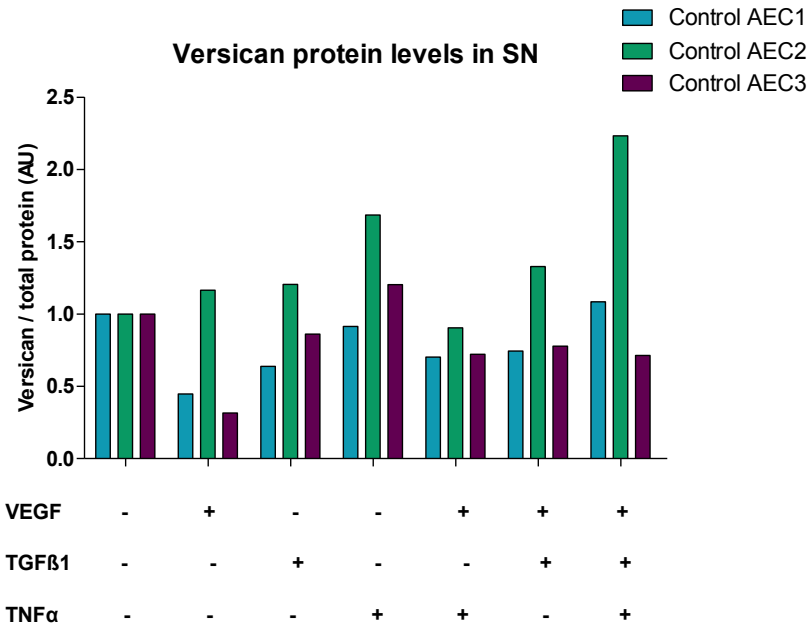

Figure 26. Effect of VEGF, TGFβ1 & TNFα on versican mRNA and protein levels of versican.

After exposure of control AEC to VEGF (10ng/ml), TGFβ1 (50pg/ml) and/or TNFα (10µg/ml), versican mRNA was determined by RT-qPCR (**a**), and protein levels of versican in supernatant (SN) were determined by ELISA (**b**).

a.

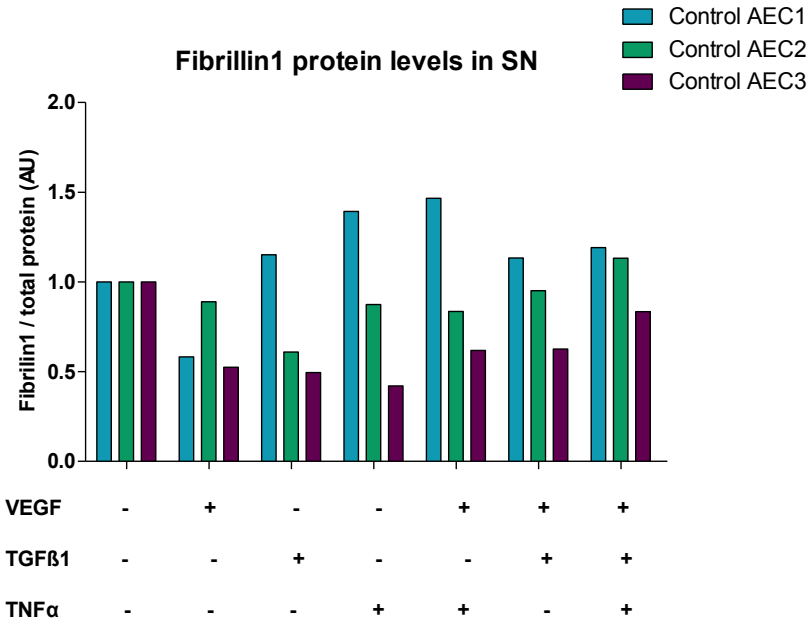

b.

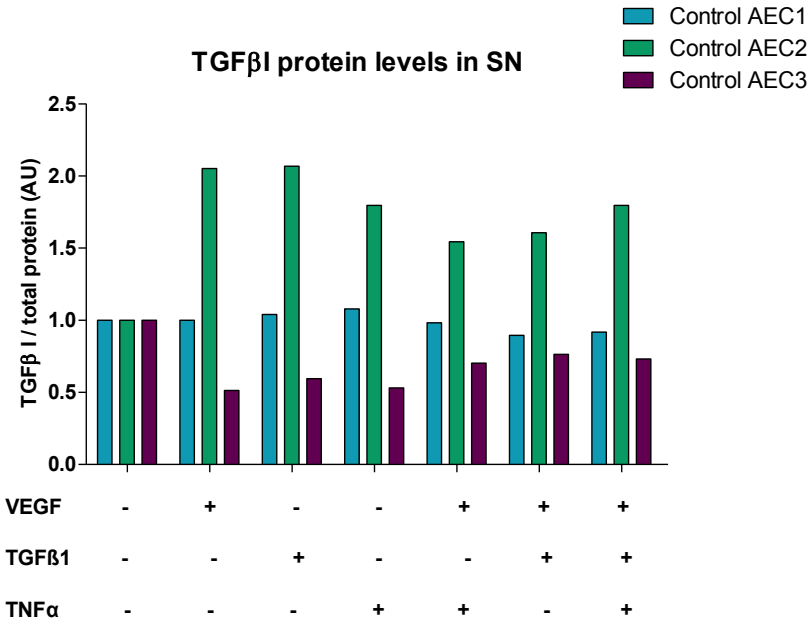

Figure 27. Effect of VEGF, TGFβ1 & TNFα on protein levels of versican fibrillin1 and TGFβI.

Effect of VEGF (10ng/ml), TGFβ1 (50pg/ml) and/or TNFα (10µg/ml) on protein levels of fibrillin1 (**a**) and TGFβI (**b**) was evaluated by ELISA in cultured supernatant of AEC.

Furthermore, tube-formation after pre-treating the cells with siRNA that targets *VCAN* was evaluated. For this, efficiency of 4 different siRNA sequences was determined, revealing that siRNA5, siRNA6 and siRNA7 decreased the expression of all 4 versican isoforms by >80% when compared to cells treated with transfection reagent DharmaFect alone (set as 100% of expression). Since siRNA5 exhibited the highest efficiency (>95%) in down-regulating *VCAN*, further experiments were performed using this siRNA. VEGF/TNFα (VT) treatment was subsequently used as a positive control for tube-formation (**Figure 28**).

Effect of human recombinant versican on tube formation was only significant after *VCAN* siRNA treatment in control AEC, while GDM AEC responded only to VEGF/TNFα stimulation (**Figure 29**). Similarly, exposure to conditioned media from control and GDM SMC had an effect on tube formation only after *VCAN* siRNA treatment (**Figure 30**).

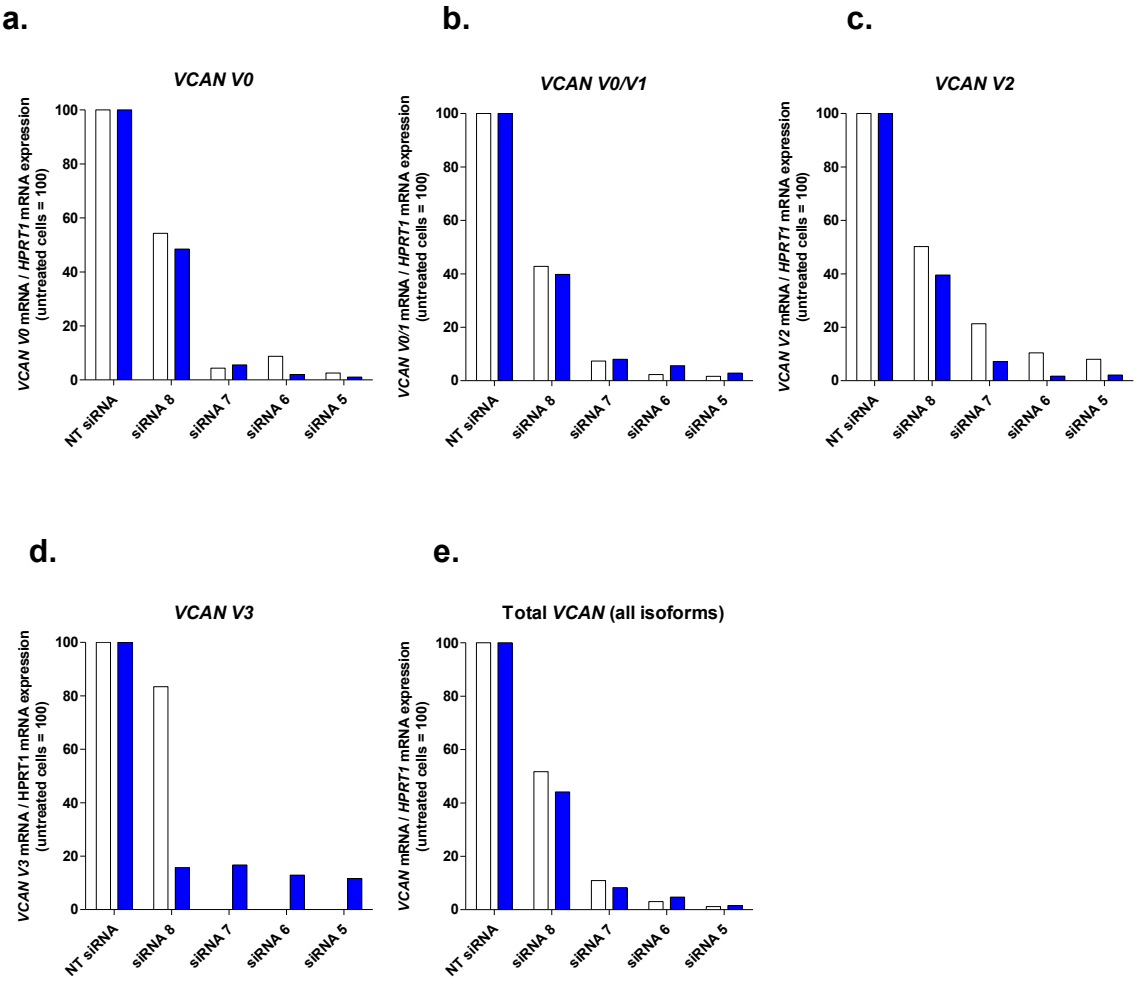

Figure 28. Efficiency evaluation of different *VCAN* siRNAs

Control and GDM AEC were treated with DharmaFect reagent but no siRNA (untreated cells), with non-targeting siRNA and 4 different siRNA against versican. ☐ Control AEC ■ GDM AEC ($n_{control\ AEC}$=1; $n_{GDM\ AEC}$=1).

a.

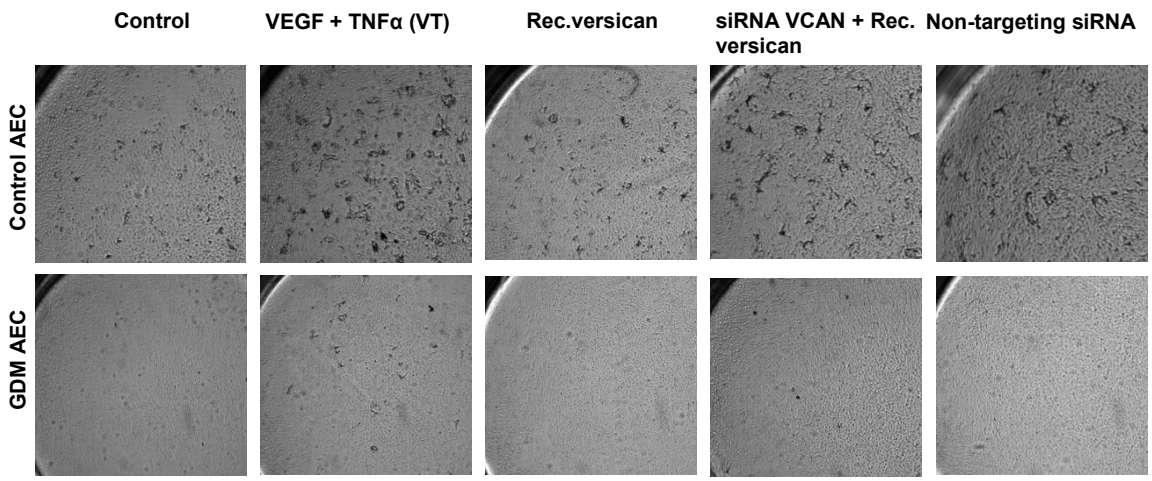

b.

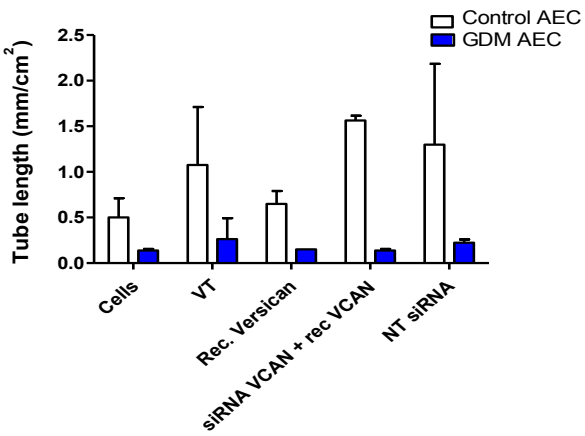

Figure 29. Effect of versican on *in vitro* tube formation of human placental AEC

In vitro tube formation of control and GDM AEC in absence or presence of VEGF + TNFα (10ng/ml and 10µg/ml, respectively) and recombinant human versican with or without previous transfection with *VCAN* siRNA (**a**) and its quantification (**b**). Quantification of pictures on 2.5X magnification was performed with Optimas 6.5. Representative pictures of quadruplicates are shown ($n_{control\ AEC}$=3; $n_{GDM\ AEC}$=2). Note: 2/4 GDM AEC isolations did not form tubes, and thus were not used in the present analysis.

a.

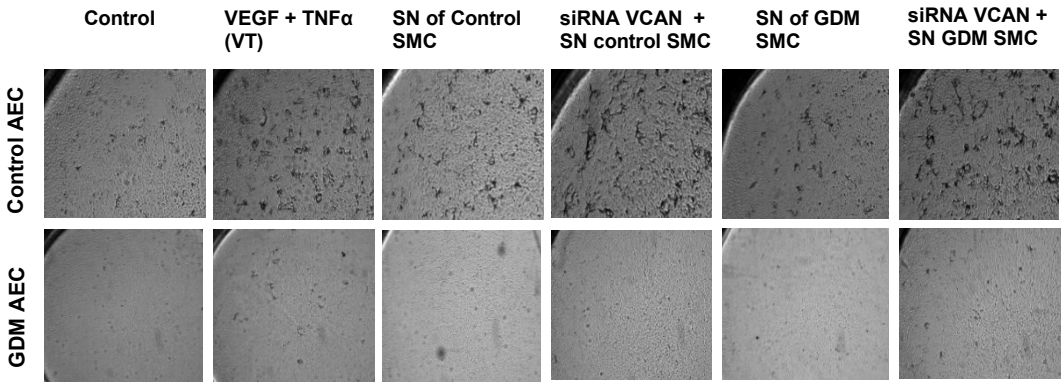

b.

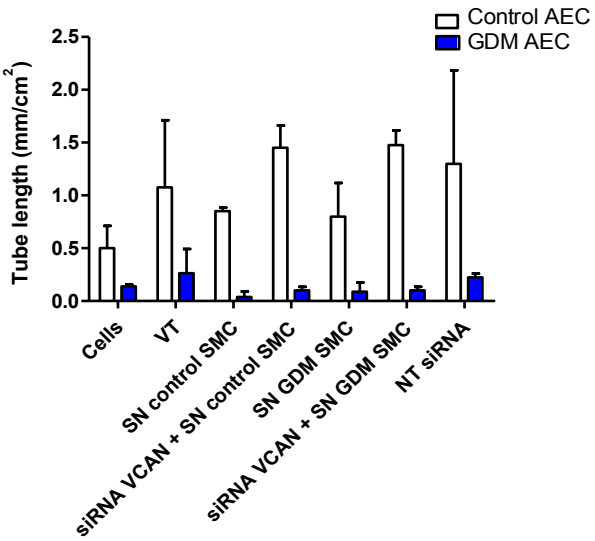

Figure 30. Effect of SMC cultured media on *in vitro* tube formation of human placental arterial endothelial cells

In vitro tube formation of control and GDM AEC in absence or presence of VEGF + TNFα (10ng/ml and 10µg/ml, respectively) and conditioned media of cultured SMC isolated from placental arteries after healthy pregnancies (control SMC) and pregnancies complicated with gestational diabetes (GDM SMC); with or without previous transfection with *VCAN* siRNA (**a**) and its quantification (**b**). Quantification of pictures on 2.5X magnification was performed with Optimas 6.5. Representative pictures of quadruplicates are shown ($n_{control\ AEC}$=3; $n_{GDM\ AEC}$=2). Note: 2/4 GDM AEC isolations did not form tubes, and thus were not used in the present analysis.

Discussion

Angiogenesis

Placental vascular development and expansion are stimulated by growth promoting and pro-angiogenic factors, such as fibroblast growth factor (FGF) and vascular endothelial growth factor (VEGF) (Cross and Claesson-Welsh, 2001). Diabetic pregnancies are associated with elevated fetal levels of FGF-2, which not only stimulate angiogenesis, but also lead to the hypercapillarization observed in placentas after pregnancies complicated with type 1 diabetes. Reports in GDM are divergent. Some studies showed increased longitudinal vascular growth and improved branching angiogenesis, possibly reflecting varied time points of GDM onset in pregnancy either within or after the complex developmental phases of vasculogenesis and angiogenesis (Desoye and Hauguel-de Mouzon, 2007). These reports support previous data obtained in our group with a Matrigel 2D-network formation assay showing that GDM AEC form more 2D-networks and longer tubes than control AEC (Cvitic, not published).

Strong immunofluorescent staining of collagen I, collagen IV and fibronectin have been reported in cryosections of first trimester and term placenta. There are reported cases suggesting that women with fibrinogen deficiencies recurrently miscarry, indicating the importance of fibrinogen-related genes (Chen and Aplin, 2003). Thus, we evaluated the capacity of control and GDM AEC to form tube-like structures using fibrinogen. And, conversely to the results using Matrigel, the use of fibrinogen on a 3D tube-formation assay showed significantly decreased tube-formation in AEC obtained from GDM placentas compared to control AEC. After seeding the cells, most GDM AEC isolations failed to migrate inside the fibrin matrix, and remained as a monolayer on top of the matrix. Interestingly, using another 3D approach using collagen as a matrix, similar results to this study were obtained (Hoch and Jantscher-Krenn, not published).

According to the manufacturer (Corning) Matrigel is a matrix preparation extracted from the Engelbreth-Holm-Swarm (EHS) mouse sarcoma, which is rich in ECM proteins. After isolation, its constitution is approximately 60% laminin, 30% collagen IV, and 8% entactin, containing also perlecan, TGFβ, EGF, insulin-like

growth factor, FGF, tissue plasminogen activator, and other growth factors present in the EHS tumor. Thus, differences obtained previously with Matrigel and the results obtained with fibrinogen might be due the presence of certain molecules in Matrigel. This matrix is not only rich in nutrients and ECM proteins, but also contains matrix metalloproteinases derived from the original tumor, which will help to degrade the matrix in order to migrate and form cellular tube-structures. Moreover, proteolytic activity of cells to enter the tissue is essential for angiogenesis to assure degradation of ECM, their migration and lumen formation within the sprouts. Proteolytic processing plays an essential role in various biological processes including angiogenesis, cell migration, cell-cycle regulation, embryonic development, wound-healing and homeostatic tissue remodeling (Ghaffari-Tabrizi-Wizsy et al., 2014)

Since endothelial proliferation and migration are key steps in angiogenesis, cell cycle proteins evaluation was of interest for this study.

Cell cycle regulators

Under the culture conditions used for a previously assessed protein array of cell cycle proteins (800000 cells with 5% FCS EBM, 37°C, 21% O_2), mRNA expression differences between control and GDM AECs were only found for *DNMT1*. Cells deprived of serum and supplements decrease their proliferation rate, and their metabolism goes to basal levels. This may explain the fact that no differences were seen between control and GDM AEC by RT-qPCR for other evaluated genes.

Immunoblot for molecules differentially expressed by protein array revealed no differences between control and GDM AEC, suggesting that protein array changes previously assessed might have been not high enough for immunoblot detection range.

Other cell cycle proteins evaluated were cyclin-dependent kinase 4 (CDK4) and cyclin-D2. Cyclin-D2 interacts with either CDK4 or CDK6 protein kinase to form a serine/threonine kinase holoenzyme complex. The regulatory component of the cyclin-D2-CDK4 complex phosphorylates and inhibits members of the retinoblastoma (RB) protein family including RB to regulate the cell-cycle during

G1/S transition. Salpeter et al. (2011) reported that cyclin-D2 is expressed at high levels in the nucleus of almost all quiescent pancreatic-cells. This high basal expression level is maintained by glucose metabolism and calcium signaling in those cells. However, there are no reports of CDK4 or cyclin-D2 expression in endothelial cells in diabetes.

We found increased *CCND2* mRNA expression by 3.4-fold in GDM compared to control AEC ($p<0.05$). Similarly, cyclin-D2 protein was increased by 45% in GDM compared to control AEC ($p<0.01$). Both mRNA and protein analysis are in concordance with higher methylation found in 5 CpGs in control AEC vs. GDM AEC, leading to decreased expression in control AEC.

In this study, CDK4 protein levels exhibited a decrease of 42% in GDM compared to control AEC ($p<0.01$). Higher methylation in 2 CpGs in GDM AEC compared to control AEC (Cvitic, not published), might be the cause of this decrease. These results are congruent with studies in mice showing that lack of CDK4 is related to insulin-deficient diabetes (Rane et al., 1999).

The activation of CDK4/CDK6 is a multistep process that requires binding to Cyclin-D (Bockstaele et al., 2009). Thus, alterations in this process, particularly decreased levels of CDK4, might be responsible for the lower proliferation rates of GDM AEC compared to control AEC previously found in our lab (Cvitic, not published). Higher methylation and decreased levels of CDK4 on transcript and protein in AEC after GDM pregnancies compared to control suggest *in utero* epigenetic programming.

Additionally, cell proliferation has also been associated to nitric oxide. NO inhibits smooth muscle cells proliferation and migration; improves proliferation and migration of endothelial cells and prevents apoptosis (Lei et al., 2013). Thus, evaluation of NO in AEC obtained from control and GDM placentas was assessed.

Nitric oxide

The effects of diabetes mellitus are extensively studied due to the growing incidence worldwide. Type 2 diabetes mellitus (T2DM) is associated with decreased NO bioavailability, elevated activation of endothelial nitric oxide synthase (eNOS) at serine 1177 and reduced flow-mediated vasodilation in diabetic patients compared to control subjects. Moreover, exposure of peripheral venous endothelial cells to insulin (10nM for 30 minutes) increased eNOS phosphorylation at serine 1177 in controls, while in cells from diabetic patients eNOS phosphorylation at serine 1177 was decreased (Montero et al., 2014; Tabit et al., 2013).

Similar findings have been found by others, reporting increased NO synthesis, eNOS transcript and protein expression, increased eNOS activity (measured by conversion of [^{3}H]-L-arginine to [^{3}H]-L-citrulline and NO) and reduced NO bioavailability in primary cultures of HUVEC isolated from pregnancies with GDM compared to controls (Westermeier et al., 2011; Di Fulvio et al., 2014).

Under our culture conditions, AEC exhibited a 2-fold tendency of upregulation in transcript levels of endothelial nitric oxide synthase after GDM compared to control ($p<0.052$). However, NO bioavailability revealed no difference between control and GDM AEC. Furthermore, control and GDM AEC responded similarly after stimulation with insulin, increasing NO availability. Pre-treatment with L-NAME (a specific inhibitor for the nitric oxide synthase) decreased intracellular NO bioavailability in both, control and GDM AEC.

Differences in eNOS transcript expression and NO bioavailability in this study from others previously reported in endothelial cells obtained from umbilical vein after GDM and in peripheral vein endothelial cells of T2DM patients might be due to the clinical characteristics of patients., or to the origin of the studied endothelial cells, which is another factor to consider in comparison between studies.

Lassance et al. (2013) confirmed phenotypic differences between endothelial cells obtained from placental veins and arteries reported previously, and also reported a differential response to key components of the surrounding environment, i.e. ECM proteins and oxygen, stating that primary human placental VEC are more sensitive to changes in the matrix composition than AEC regarding proliferation,

viability and survival. This explains differences found in this study with previous reports.

Endothelial function alterations occur together with modifications in endothelial phenotype, which, among other factors, is determined by the expression of cell adhesion molecules. There are 2 classes of adhesion molecules shown to be a useful marker of endothelial dysfunction (Kurt et al., 2010): selectins and the molecules of the immunoglobulin superfamily, mainly intercellular cell adhesion molecule-1 (ICAM-1) and vascular cell adhesion molecule-1 (VCAM-1) (Fotis et al., 2012). After proteolytic cleavage, soluble forms of these molecules are released: sICAM-1, sVCAM-1 and sE-selectin.

Reports of cell adhesion molecules' evaluation in GDM are assorted. sICAM-1 and sVCAM-1 have been reported to be increased in plasma of women with GDM compared to women with normal glucose tolerance (NGT). sICAM-1 showed no difference in serum samples and CBS of GDM and NGT women; whereas sVCAM was found to be increased in maternal serum and CBS of GDM vs. non-GDM pregnancies and plasma levels of E-selectin showed no difference between these groups (Kautsky-Willer et al., 1997; Mordwinkin et al., 2013; Telejko et al., 2009).

No differences were found in ICAM-1 and VCAM-1 placental mRNA expression or in supernatant of cultured placental explants of NGT and GDM pregnancies (Lappas, 2014). Immunohistochemistry for evaluating ICAM-1 expression showed no difference in umbilical artery, vein or placental from GDM vs. non GDM pregnancies (Kurt et al., 2010; Babawale et al., 2000). Di Fulvio et al. (2014) reported increased ICAM-1 and VCAM-1 in HUVEC obtained from GDM compared to controls, while other reports showed increase in mRNA level and bound-protein levels of ICAM-1 and E-selectin; and no differences in bound protein or mRNA levels of VCAM-1 (Giri et al., 2013). Furthermore, Steinborn (1999) reported non-detectable levels of VCAM-1 and E-selectin in endothelial cells of fetal vasculature, in which just ICAM-1 was found.

In the present study, no changes in mRNA or total protein levels of cell adhesion molecules were found between control and GDM AEC. However, GDM AEC exhibited a decrease in membrane-bound ICAM-1 levels compared to control

AEC. No changes in sICAM-1 levels in CBS or in supernatant of cultured control and GDM AEC were found. Additionally, analysis of ICAM-1 in placental tissue by immunohistochemistry revealed a weaker signal in GDM vs. control placental tissue. These results were surprising, but are concordant with decreased levels of ICAM-1 in the endothelial compartment of GDM placentas by immunohistochemistry reported by Kurt et al. (2010).

Cell adhesion molecules play a crucial role in binding and activating leukocytes during inflammation, and thus, their study in placental vasculature is of great interest. Since only changes in ICAM-1 were found, placental tissue sections were stained in order to identify cells interacting with ICAM-1. Immunohistochemistry using antibodies against ICAM-1 binding partners CD11a and CD18 revealed positive staining of CD11a fetal blood cells, while CD18 was positive in fetal blood cells and Hofbauer cells, suggesting that ICAM-1 mediated cell-cell interaction might occur through these cells (Díaz-Pérez et al., 2016).

Furthermore, NO not only controls vascular tone, cellular proliferation and inflammation (Deanfield et al., 2007), but it can also inhibit leukocyte adhesion to the vessel wall by either diminishing the capacity of CD11/CD18 to bind to the endothelial cell surface or by inhibiting CD11/CD18 expression on leukocytes (Förstermann and Li, 2011).

Due to the importance of extracellular matrix degradation for angiogenesis, and since versican differences between control and GDM AEC appeared to be the most significant molecule when studying the transcriptome of these cells, further evaluation of versican and its binding partners fibrillin1 and TGFβI was of interest.

ECM: versican and binding partners

Total versican mRNA expression was found to be higher in GDM AEC compared to control AEC. This was accounted not only by higher *VCAN V0* mRNA expression in GDM AEC, but also by *VCAN V3*, which was only detected in GDM AEC. While total protein levels of versican exhibited no change in cell lysates, lower levels were found in supernatant of cultured GDM AEC compared to controls. The opposite was found for the versican isoform V0: increased levels in cell lysates of GDM AEC vs. control

AEC, while no difference was found between supernatant of control AEC and supernatant of GDM AEC. These differences indicate changes in expression, translation and secretion of different isoforms of versican.

Overexpression of versican V3, which lacks chondroitin sulfate chains, has been reported to alter arterial smooth muscle cell phenotype by enhancing cell adhesion and by diminishing growth and migration. Therefore, versican V3 appears to compete for binding sites with other versican isoforms that contain chondroitin sulfate chains linked to hyaluronan on the cell surface. (Chan et al., 2010; Wight 2002). Thus, versican changes observed may explain the differences in migration and proliferation found in AEC isolated after GDM pregnancies vs. control pregnancies (Cvitic, Nussbaumer, Hiden, not published)

In regards to versican and its binding partners, TGFβI and FBN1 have increased mRNA levels in AEC exposed to GDM. However, whilst the higher expression translates to more protein synthesis only for TGFβI and FBN1, versican was not detected by immunoblot or immunofluorescence of cultured cells. This indicates that levels of versican under our culture conditions are too low to be detected by this techniques, which was corroborated by [^{35}S]-proteoglycan synthesis analysis, suggesting that both control and GDM derived AEC fail to produce/secrete detectable amounts of versican under culture conditions. This confirms previous observations showing that resting endothelial cells from different tissues transcribe several isoforms of versican, but fail to translate mRNA into detectable protein levels under basal conditions (Cattaruzza et al., 2002).

Furthermore, versican plays a role in tissue remodeling of the ECM that is associated with developmental events in human pregnancy, such as involution and rearrange of cervical connective tissue. Increased versican in this tissue during pregnancy has been found, reaching its highest concentration in the ripe cervix instantly after vaginal delivery, and decreases notoriously during the involution process (Wight, 2002). We found that, while expression of isoforms V2 and V3 did not change between first trimester and term placental tissue, expression of *VCAN* V0 in term placental tissue decreased by 78% compared to first trimester placental tissue. These data confirm the importance of versican, and in particular of isoform V0 in human placental development.

When evaluating the effect of recombinant versican V3 in angiogenesis after downregulating *VCAN* gene targeting all isoforms, *VCAN* siRNA treatment had an effect on the response of cells to recombinant versican. Similarly, increased tube-formation was observed after stimulating cells with supernatant of cultured SMC obtained from control and GDM human term placentas previously treated with *VCAN* siRNA, suggesting that siRNA treatment has an effect itself on angiogenesis, which has not yet been elucidated (Kalluri and Kanasaki, 2008), increasing the difficulty to comprehend these data.

Altogether, alterations found in extracellular matrix protein versican, in cell cycle regulators CDK4 and cyclin-D2, and in the angiogenic potential of AEC after GDM might be compensated with unchanged NO bioavailability and eNOS transcript expression, together with decreased levels of ICAM-1 and unaltered levels of the other cell adhesion molecules, which appear to have a protective role of the placenta in gestational diabetes mellitus.

References

- Babawale, M.O., Lovat, S., Mayhew, T.M., Lammiman, M.J., James, D.K., Leach, L. (2000). Effects of gestational diabetes on junctional adhesion molecules in human term placental vasculature. *Diabetologia*, 43(9), pp. 1185-1196.

- Blaschitz, A., Gauster, M., Dohr, G. (2008). Application of cryo-compatible antibodies to human placenta paraffin sections. *Histochemistry and Cell Biology*, 130, pp. 595-599.

- Bockstaele, L., Bisteau, X., Paternot, S., Roger, P.P. (2009). Differential regulation of cyclin-dependent kinase 4 (CDK4) and CDK6, evidence that CDK4 might not be activated by CDK7, and design of a CDK6 activating mutation. *Molecular and Cellular Biology*, 29(15), pp. 4188-4200.

- Buckley, B.S., Harreiter, J., Damm, P., Corcoy, R., Chico, A., Simmons, D., Vellinga, A., Dunne, F.; DALI Core Investigator Group. (2012). Gestational diabetes mellitus in Europe: prevalence, current screening practice and barriers to screening. *Diabetic Medicine*, 29(7), pp. 844-854.

- Bustin S.A. (2002). Quantification of mRNA using real-time reverse transcription PCR (RTPCR): trends and problems. *Journal of Molecular Endocrinology*, 29, pp. 23-39.

- Bustin S.A. (2005). Quantitative real-time RT-PCR - a perspective. *Journal of Molecular Endocrinology*, 34, pp. 597-601.

- Cattaruzza, S., Schiappacassi, M., Ljungberg-Rose, A., Spessotto, P., Perissinotto, D., Mörgelin, M., Mucignat, M.T., Colombatti, A., Perris, R. (2002). Distribution of PG-M/versican variants in human tissues and de novo expression of isoform V3 upon endothelial cell activation, migration, and neoangiogenesis in vitro. *Journal of Biological Chemistry*, 277(49), pp. 47626-47635.

- Chan, C.K., Rolle, M.W., Potter-Perigo, S., Braun, K.R., Van Biber, B.P., Laflamme, M.A., Murry, C.E., Wight T.N. (2010). Differentiation of cardiomyocytes from human embryonic stem cells is accompanied by changes in the extracellular matrix production of versican and hyaluronan. *Journal of Cellular Biochemistry*, 111(3), pp. 585-596.

- Chen, C.P., Aplin, J.D. (2003). Placental extracellular matrix: gene expression, deposition by placental fibroblasts and the effect of oxygen. *Placenta*, 24(4), pp. 316-325.

- Chistiakov, D.A., Revin, V.V., Sobenin, I.A., Orekhov, A.N., Bobryshev, Y.V. (2015). Vascular endothelium: functioning in norm, changes in atherosclerosis and current dietary approaches to improve endothelial function. *Mini Reviews in Medicinal Chemistry*, 15(4), pp. 338-350.

- Cross, M.J., Claesson-Welsh, L. (2001). FGF and VEGF function in angiogenesis: signalling pathways, biological responses and therapeutic inhibition. *Trends in Pharmacological Sciences*, 22(4), pp. 201-207.

- Cummings, B. (2005). Placental circulation. *Pearson Education, Inc*. [online] Available at: http://science.kennesaw.edu/~jdirnber/Bio2108/Lecture/LecPhysio/46-17-PlacentalCirculat-AL.jpg)

- Davignon, J., Ganz, P. (2004). Role of endothelial dysfunction in atherosclerosis. *Circulation*, 109(23 Suppl 1), pp. III27-III32.

- Deanfield, J.E., Halcox, J.P., Rabelink, T.J. (2007). Endothelial function and dysfunction: testing and clinical relevance. *Circulation*, 115(10), pp. 1285-1295.

- Desoye, G., Hauguel-de Mouzon, S. (2007). The human placenta in gestational diabetes mellitus. The insulin and cytokine network. *Diabetes Care*, 30(Suppl 2), pp. S120-S126.

- Di Fulvio. P., Pandolfi, A., Formoso, G., Di Silvestre, S., Di Tomo, P., Giardinelli, A., De Marco, A., Di Pietro, N., Taraborrelli, M., Sancilio, S., Di Pietro, R., Piantelli, M., Consoli, A. (2014). Features of endothelial dysfunction in umbilical cord vessels of women with gestational diabetes. Nutrition, *Metabolism and Cardiovascular Diseases*, 24(12), pp. 1337-1345.

- Díaz-Pérez, F.I., Hiden, U., Gauster, M., Lang, I., Konya, V., Heinemann, A., Lögl, J., Saffery, R., Desoye, G., Cvitic, S. (2016). Post-transcriptional down regulation of ICAM-1 in feto-placental endothelium in GDM. *Cell Adhesion and Migration*, 10(1-2), pp. 18-27.

- Dunn, J., Thabet, S., Jo, H. (2015). Flow-Dependent Epigenetic DNA Methylation in Endothelial Gene Expression and Atherosclerosis. *Arteriosclerosis, Thrombosis, and Vascular Biology*, 35(7), pp.1562-1569.

- Edwards, I.J. (2012). Proteoglycans in prostate cancer. *Nature Reviews Urology*, 9(4), pp. 196-206.

- Förstermann, U., Li, H. (2011). Therapeutic effect of enhancing endothelial nitric oxide synthase (eNOS) expression and preventing eNOS uncoupling. *British Journal of Pharmacology*, 164(2), pp. 213-223.

- Fotis, L., Giannakopoulos, D., Stamogiannou, L., Xatzipsalti, M. (2012). Intercellular cell adhesion molecule-1 and vascular cell adhesion molecule-1 in children. Do they play a role in the progression of atherosclerosis? *Hormones (Athens)*, 11(2), pp. 140-146.

- Ghaffari-Tabrizi-Wizsy, N., Cvitic, S., Tam-Amersdorfer, C., Bilban, M., Majali-Martinez, A., Schramke, K., Desoye, G., Hiden, U. (2014). Different Preference of Degradome in Invasion versus Angiogenesis. *Cells Tissues Organs*, 200 (3-4), pp. 181-194.

- Giachini, F.R.C., Carriel, V., Capelo, L.P., Tostes, R.C., Carvalho, M.H., Fortes, Z.B., Zorn, T.M., and San Martin, S. (2008). Maternal diabetes affects specific extracellular matrix components during placentation. *Journal of Anatomy*, 212(1), pp. 31-41.

- Giri, H., Chandel, S., Dwarakanath, L.S., Sreekumar, S., Dixit, M. (2013). Increased endothelial inflammation, sTie-2 and arginase activity in umbilical cords obtained from gestational diabetic mothers. *PLoS One*, 8(12): e84546.

- Gude, N.M., Roberts, C.T., Kalionis, B., King, R.G. (2004). Growth and function of the normal human placenta. *Thrombosis Research*, 114(5-6), pp. 397-407.

- Hiden, U., Wadsack, C., Prutsch, N., Gauster, M., Weiss, U., Frank, H.-G., … Desoye, G. (2007). The first trimester human trophoblast cell line ACH-3P: A novel tool to study autocrine/paracrine regulatory loops of human trophoblast subpopulations – TNF-α stimulates MMP15 expression. *BMC Developmental Biology*, 7, pp. 137.

- Huang P.L. (2003). Endothelial nitric oxide synthase and endothelial dysfunction. *Current Hypertension Reports*, 5 (6), pp. 473-480.

- Kalluri, R., Kanasaki, K. (2008). RNA interference: generic block on angiogenesis. *Nature*, 452(7187), pp. 543-545.

- Kautzky-Willer, A., Fasching, P., Jilma, B., Waldhäusl, W., Wagner, O.F. (1997). Persistent elevation and metabolic dependence of circulating E-selectin after delivery in women with gestational diabetes mellitus. *The Journal of Clinical Endocrinology and Metabolism*, 82(12), pp. 4117-4121.

- Koolwijk, P., van Erck, M.G., de Vree, W.J., Vermeer, M.A., Weich, H.A., Hanemaaijer, R., van Hinsbergh, V.W. (1996). Cooperative effect of TNFalpha, bFGF, and VEGF on the formation of tubular structures of human microvascular endothelial cells in a fibrin matrix. Role of urokinase activity. *Journal of Cell Biology*, 132(6), pp. 1177-1188.

- Kurt, M., Zulfikaroglu, E., Ucankus, N.L., Omeroglu, S., Ozcan, U. (2010). Expression of intercellular adhesion molecule-1 in umbilical and placental vascular tissue of gestational diabetic and normal pregnancies. *Archives of Gynecology and Obstetrics*, 281(1), pp. 71-76.

- Lang, I., Schweizer, A., Hiden, U., Ghaffari-Tabrizi, N., Hagendorfer, G., Bilban, M., Pabst, M.A., Korgun, ET., Dohr, G., Desoye, G. (2008). Human fetal placental endothelial cells have a mature arterial and a juvenile venous phenotype with adipogenic and osteogenic differentiation potential. *Differentiation*, 76(10), pp.1031-1043.

- Lappas, M. (2014). Markers of endothelial cell dysfunction are increased in human omental adipose tissue from women with pre-existing maternal obesity and gestational diabetes. *Metabolism*, 63(6), pp. 860-873.

- Lassance, L., Miedl, H., Absenger, M., Diaz-Perez, F., Lang, U., Desoye, G., Hiden, U. (2013). Hyperinsulinemia stimulates angiogenesis of human fetoplacental endothelial cells: a possible role of insulin in placental hypervascularization in diabetes mellitus. *The Journal of Clinical Endocrinology and Metabolism*, 98(9), pp. E1438-E1447.

- Lee, J.Y., Kong, G. (2016). Roles and epigenetic regulation of epithelial-mesenchymal transition and its transcription factors in cancer initiation and progression. *Cellular and Molecular Life Sciences*, pp. 1-18

- Lehnen, H., Zechner, U., Haaf, T. (2013). Epigenetics of gestational diabetes mellitus and offspring health: the time for action is in early stages of life. *Molecular Human Reproduction*, 19(7), pp. 415-422.

- Lei, J., Vodovotz, Y., Tzeng, E., Billiar, T.R. (2013). Nitric oxide, a protective molecule in the cardiovascular system. *Nitric Oxide*, 35, pp. 175-185.
- Loegl, J., Nussbaumer, E., Hiden, U., Majali-Martinez, A., Ghaffari-Tabrizi-Wizy, N., Cvitic, S., Lang, I, Desoye, G and Huppertz, B. (2016). Pigment epithelium-derived factor (PEDF): a novel trophoblast-derived factor limiting feto-placental angiogenesis in late pregnancy. *Angiogenesis*, 19, pp. 373-388.
- Mathew, V., Ayyar, S.V. (2013). Developmental origins of adult diseases. *Indian Journal of Endocrinology and Metabolism*, 16(4), pp. 532-541.

- Michiels, C. (2003). Endothelial cell functions. *Journal of Cellular Physiology*, 196(3), pp. 430-443.

- Montero, D., Walther, G., Stehouwer, C.D., Houben, A.J., Beckman, J.A., Vinet, A. (2014). Effect of antioxidant vitamin supplementation on endothelial function in type 2 diabetes mellitus: a systematic review and meta-analysis of randomized controlled trials. *Obesity Reviews*, 15(2), pp. 107-116.

- Mordwinkin, N.M., Ouzounian, J.G., Yedigarova, L., Montoro, M.N., Louie, SG., Rodgers, K.E. (2013). Alteration of endothelial function markers in women with gestational diabetes and their fetuses. *Journal of Maternal-Fetal and Neonatal Medicine*, 26(5), pp. 507-512.

- Pal, S., Tyler, J.K. (2016). Epigenetics and aging. *Science Advances*, 2(7): e1600584

- Piñon, R. (2002). *University Science Books*, pp. 298-303

- Pleiner, J., Mittermayer, F., Langenberger, H., Winzer, C., Schaller, G., Pacini, G., Kautzky-Willer, A., Tura, A., Wolzt, M. (2007). Impaired vascular nitric oxide bioactivity in women with previous gestational diabetes. *Wiener klinische Wochenschrift*, 119(15-16), pp. 483-489.

- Rama, S., Rao, A.J. (2003). Regulation of growth and function of the human placenta. *Molecular and Cellular Biochemistry*, 253(1-2), pp. 263-268.

- Rane, S.G., Dubus, P., Mettus, R.V., Galbreath, E.J., Boden, G., Reddy, E.P., Barbacid, M. (1999). Loss of Cdk4 expression causes insulin-deficient diabetes and Cdk4 activation results in beta-islet cell hyperplasia. *Nature Genetics*, 22(1), pp. 44-52.

- Salpeter, S.J., Klochendler, A., Weinberg-Corem, N., Porat, S., Granot, Z., Shapiro, A.M., Magnuson, M.A., Eden, A., Grimsby, J., Glaser, B., Dor, Y. (2011). Glucose regulates cyclin D2 expression in quiescent and replicating pancreatic β-cells through glycolysis and calcium channels. *Endocrinology*, 152(7), pp. 2589-2598.

- Searle, A., Gómez-Rosso, L., Meroño, T., Salomon, C., Durán-Sandoval, D., Giunta, G., Grant, C., Calvo, C., Lamperti, L., Brites, F., Aguayo, C. (2011). High LDL levels are associated with increased lipoprotein-associated phospholipase A(2) activity on nitric oxide synthesis and reactive oxygen species formation in human endothelial cells. *Clinical Biochemistry*, 44(23), pp. 171-177.

- Sobrevia, L., Salsoso, R., Sáez, T., Sanhueza, C., Pardo, F., Leiva, A. (2015). Insulin therapy and fetoplacental vascular function in gestational diabetes mellitus. *Experimental Physiology*, 100(3), pp. 231-238.

- Steinborn, A., Sohn, C., Heger, S., Niederhut, A., Hildenbrand, R., Kaufmann, M. (1999). Labour-associated expression of intercellular adhesion molecule-1 (ICAM-1) in placental endothelial cells indicates participation of immunological processes in parturition. *Placenta*, 20(7), pp. 567-573.

- Su, E.J. (2015). Role of the fetoplacental endothelium in fetal growth restriction with abnormal umbilical artery Doppler velocimetry. *American Journal of Obstetrics and Gynecology,* 213(4 Suppl), pp. S123-S130.

- Tabit, C.E., Shenouda, S.M., Holbrook, M., Fetterman, J.L., Kiani, S., Frame, A.A., Kluge, M.A., Held, A., Dohadwala, M.M., Gokce, N., Farb, M.G., Rosenzweig, J., Ruderman, N., Vita, J.A., Hamburg, N.M. (2013). Protein kinase C-β contributes to impaired endothelial insulin signaling in humans with diabetes mellitus. *Circulation*, 127(1), pp. 86-95.

- Telejko, B., Zonenberg, A., Kuzmicki, M., Modzelewska, A., Niedziolko-Bagniuk, K., Ponurkiewicz, A., Nikolajuk, A., Gorska, M. (2009). Circulating asymmetric

dimethylarginine, endothelin-1 and cell adhesion molecules in women with gestational diabetes. *Acta Diabetologica*, 46(4), pp. 303-308.

- Tousoulis, D., Kampoli, A.M., Tentolouris, C., Papageorgiou, N., Stefanadis, C. (2012). The role of nitric oxide on endothelial function. *Current Vascular Pharmacology*, 10(1), pp. 4-18.

- van Hinsbergh, V.W., Collen, A., Koolwijk, P. (1999). Angiogenesis and anti-angiogenesis: perspectives for the treatment of solid tumors. *Annals of Oncology*, 10(Suppl 4), pp. 60-63.

- van Hinsbergh, V.W., Collen, A., Koolwijk, P. (2001). Role of fibrin matrix in angiogenesis. *Annals of the New York Academy of Sciences*, 936, pp. 426-437.

- Vrachnis, N., Antonakopoulos, N., Iliodromiti, Z., Dafopoulos, K., Siristatidis, C., Pappa, KI., Deligeoroglou, E., Vitoratos, N. (2012). Impact of maternal diabetes on epigenetic modifications leading to diseases in the offspring. *Experimentals Diabetes Research*, 2012, 538474.

- Wadsack, C., Desoye, G., Hiden, U. (2012). The feto-placental endothelium in pregnancy pathologies. *Wiener Medizinische Wochenschrift*, 162(9-10), pp. 220-224.

- Westermeier F, Salomón C, González M, Puebla C, Guzmán-Gutiérrez E, Cifuentes F, Leiva A, Casanello P, Sobrevia L. 2011. Insulin restores gestational diabetes mellitus-reduced adenosine transport involving differential expression of insulin receptor isoforms in human umbilical vein endothelium. *Diabetes*, 60(6), pp. 1677-1687.

- Wight, T. N., Kinsella, M.G., Evanko, S.P., Potter-Perigo, S., & Merrilees, M.J. (2014). Versican and the Regulation of Cell Phenotype in Disease. *Biochimica et Biophysica Acta*, 1840(8), pp. 2441–2451.

- Wight, T.N. (2002). Versican: a versatile extracellular matrix proteoglycan in cell biology. *Current Opinion in Cell Biology*, 14(5), pp. 617-623.

- Wight, T.N., Merrilees, M.J. (2004). Proteoglycans in atherosclerosis and restenosis: key roles for versican. *Circulation Research*, 94, pp. 1158-1167

- Wu, Y.J., La Pierre, D.P., Wu, J., Yee, A.J., Yang, B.B. (2005). The interaction of versican with its binding partners. *Cell Research*, 15(7), pp. 483-494.